Ratiometric fluorescence sensing of D-allulose using inclusion complex of γ-cyclodextrin with benzoxaborole-based probe

Yota Suzuki,* [a] Takeshi Hashimoto,[a] Takashi Hayashita* [a]

a. Department of Materials and Life Sciences, Faculty of Science and Technology, Sophia University, 7-1, Kioi-cho, Chiyoda-ku, Tokyo, 102-8554 (Japan)

Table of Contents

Experimental details

Reagents

Methyl 4-bromo-3-methylbenzoate (*1a*, Tokyo Chemical Industries), bis(pinacolato)diboron (Tokyo Chemical Industries), potassium acetate (Fujifilm Wako Chemicals), Pd(dppf)Cl$_2 \cdot$CH$_2$Cl$_2$ (Tokyo Chemical Industries), n-bromosuccinimide (NBS, Fujifilm Wako Chemicals), 2,2'-azobis(isobutyronitrile) (AIBN, Fujifilm Wako Chemicals), hydrochloric acid (Fujifilm Wako Chemicals), sodium hydroxide (Fujifilm Wako Chemicals), 1-aminopyrene (Tokyo Chemical Industries), 4-(4,6-dimethoxy-1,3,5-triazin-2-yl)-4-methylmorpholinium chloride (DMT-MM, Tokyo Chemical Industries), 1,3-dihydro-1-hydroxy-2,1-benzoxaborole-6-carboxylic acid (*1-COOH*, Toronto Research Chemicals), all dehydrated solvents (Kanto Chemical Industry), silica-gel 60 (Merck Millipore), magnesium sulfate (Fujifilm Wako Chemicals), dimethyl sulfoxide-d$_6$ (DMSO-d$_6$, Kanto Chemical Industry), deuterium oxide (D$_2$O, Kanto Chemical Industry), and 35% deuterium chloride solution in D$_2$O (35% DCl, Fujifilm Wako Chemicals) were used as received from commercial resources. 1,3-dihydro-1-hydroxy-2,1-benzoxaborole-5-carboxylic acid (*2-COOH*) was synthesised according to the literature method.[1] Dimethyl sulfoxide (DMSO, Luminasol®, Dojindo Laboratories), 50% sodium hydroxide solution (super special grade, Fujifilm Wako Chemicals), sodium chloride (Fujifilm Wako Chemicals), disodium hydrogen phosphate (Fujifilm Wako Chemicals), *β*-cyclodextrin (Kanto Chemical Industry), *γ*-cyclodextrin (Kanto Chemical Industry), D-fructose (Fujifilm Wako Chemicals), D-glucose (Fujifilm Wako Chemicals), D-galactose (Fujifilm Wako Chemicals), D-allulose (Tokyo Chemical Industries) and milli-Q water were used for spectroscopic measurements.

Synthesis of 2-COOH
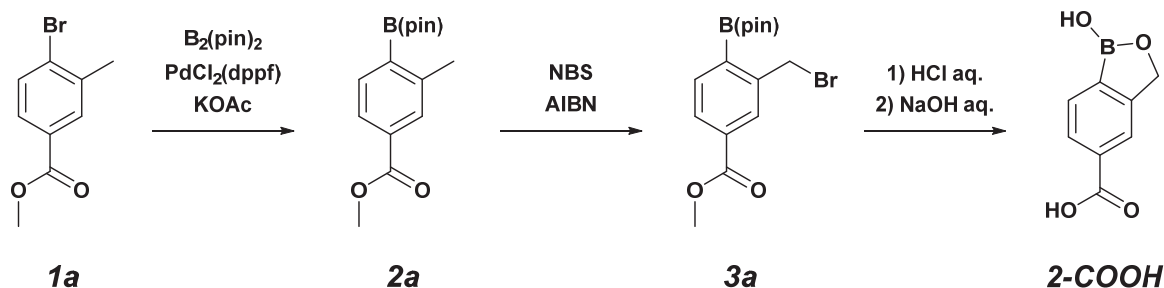
Scheme S1. Synthetic routes of *2-COOH*.

2-COOH was synthesised by following to the literature method.[1]

Preparing a sample solution for the measurement of nuclear overhauser effect spectroscopy (NOESY) spectrum

The pD of D_2O solution containing 10 mM carbonate buffer was adjusted with 35% DCl. The pH value read by the pH meter (pH_{read}) was corrected to pD value according to the equation: $pD = pH_{read} + 0.4$.[2] γ-cyclodextrin was dissolved in the buffered D_2O solution. 0.48 mL of the γ-cyclodextrin D_2O solution and 0.12 mL of 10 mM probe DMSO-d_6 solution were mixed.
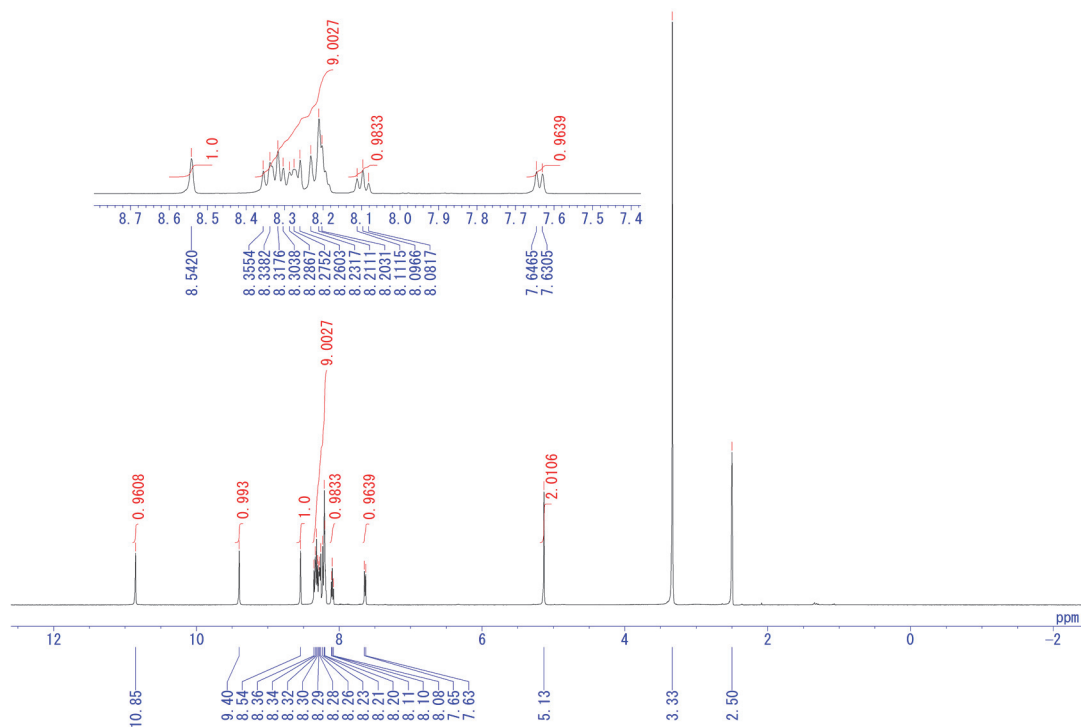
NMR spectra

12/Suzukiyo_211004_SP029_1H

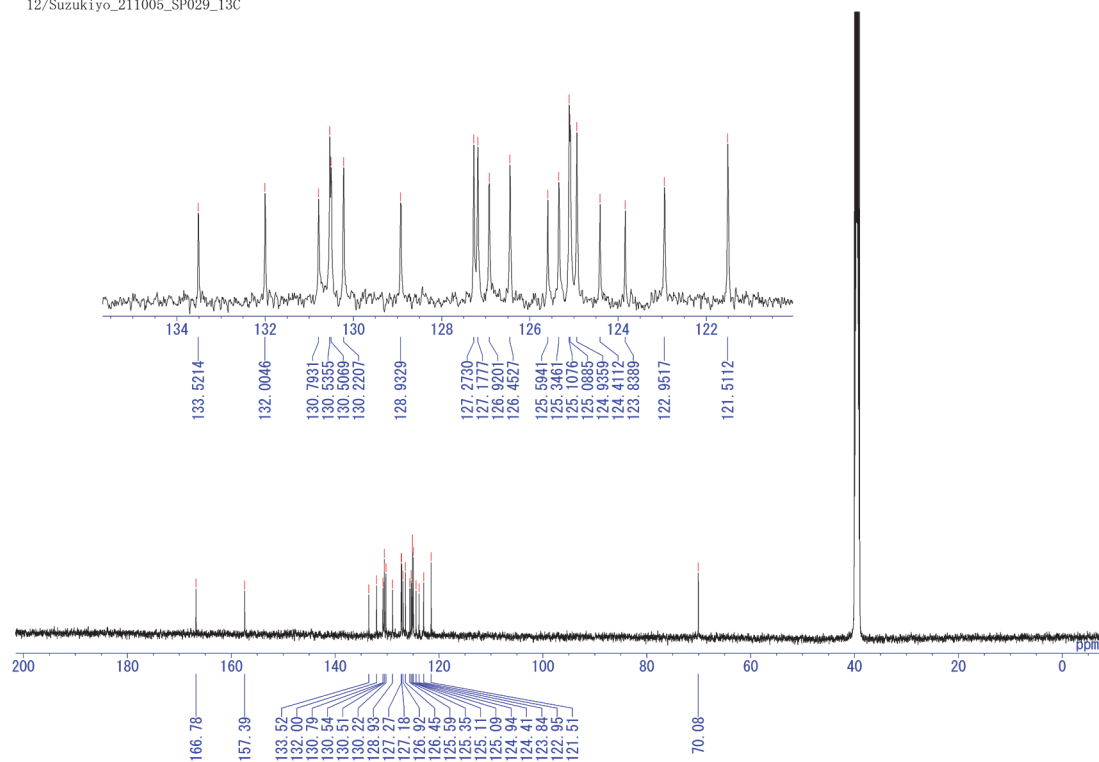Figure S1-1. ^{1}H NMR spectrum of *1* in DMSO-d$_6$.

12/Suzukiyo_211005_SP029_13C

Figure S1-2. ^{13}C NMR spectrum of *1* in DMSO-d$_6$.

Figure S1-3. ¹H NMR spectrum of **2** in DMSO-d₆.

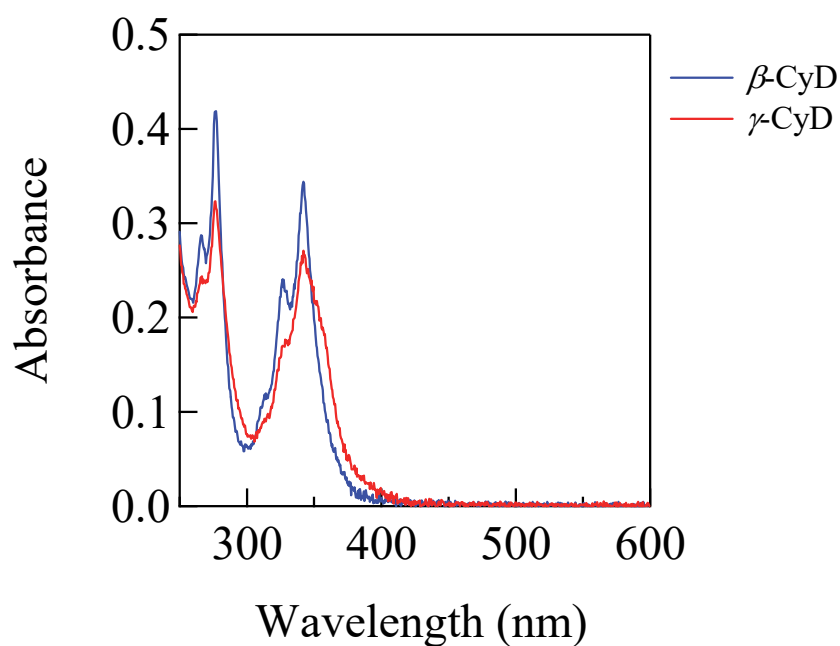Figure S1-4. ¹³C NMR spectrum of **2** in DMSO-d₆.

Figure S2-1. UV-vis absorption spectra of **1** (10.3 µM) in the presence of 5 mM _β_-CyD (blue) and _γ_-CyD (red) in DMSO/water (2/98 in v/v): 10 mM of phosphate buffer, pH = 9, _T_ = 25°C, and _I_ = 0.10 M.
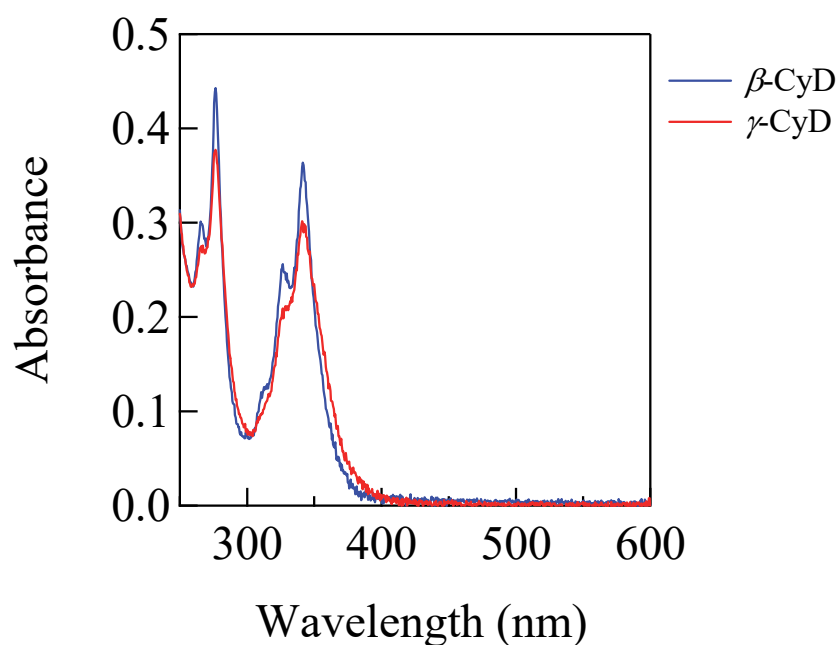

Figure S2-2. UV-vis absorption spectra of **2** (11.3 µM) in the presence of 5 mM _β_-CyD (blue) and _γ_-CyD (red) in DMSO/water (2/98 in v/v): 10 mM of phosphate buffer, pH = 9, _T_ = 25°C, and _I_ = 0.10 M.
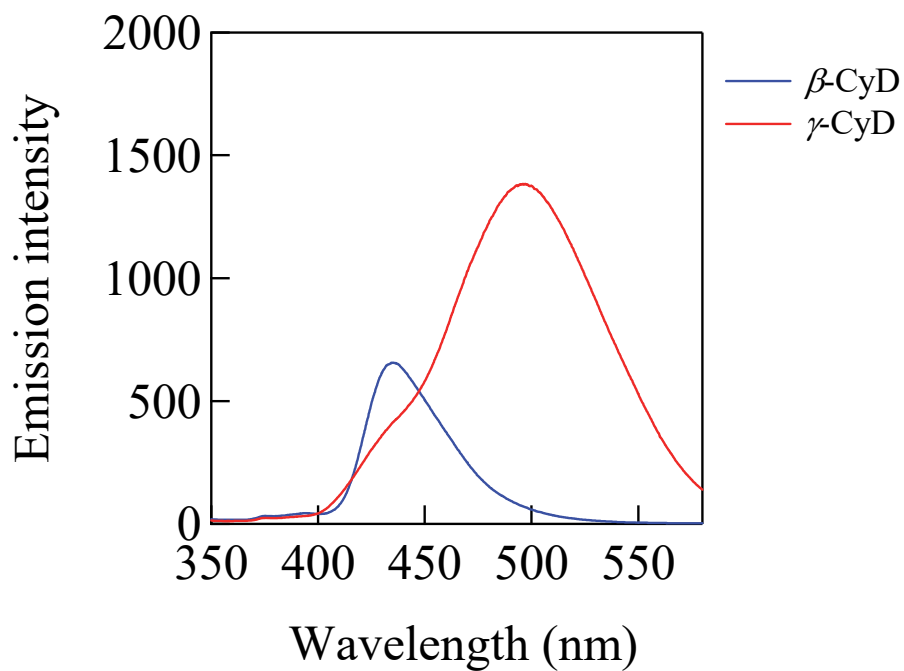
Figure S3-1. Fluorescence spectra of **1** (10.3 µM) in the presence of 5 mM β-CyD (blue) and γ-CyD (red) in DMSO/water (2/98 in v/v): 10 mM of phosphate buffer, pH = 9, T = 25°C, I = 0.10 M, and λ_{ex} = 305 nm.
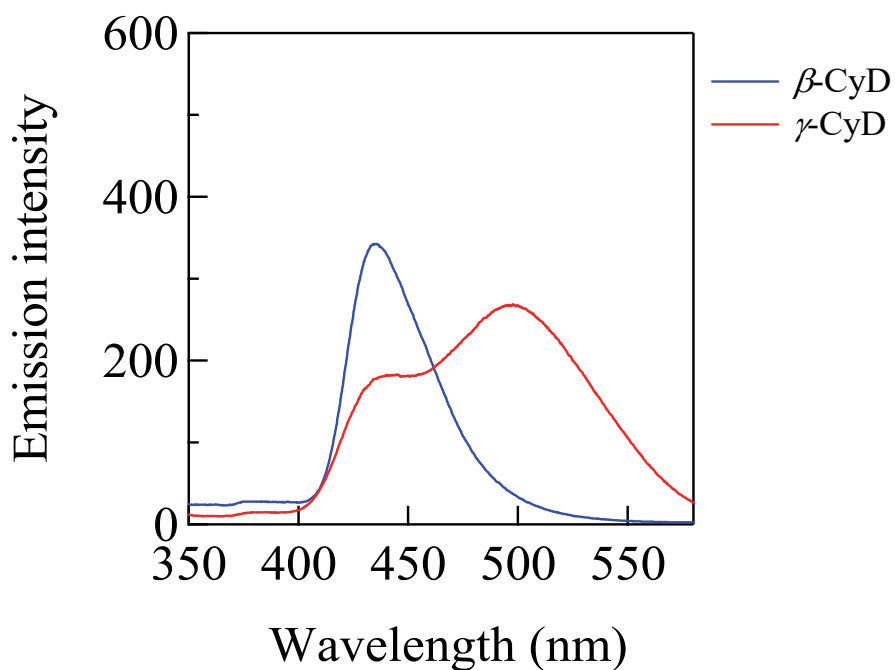

Figure S3-2. Fluorescence spectra of **2** (11.3 µM) in the presence of 5 mM β-CyD (blue) and γ-CyD (red) in DMSO/water (2/98 in v/v): 10 mM of phosphate buffer, pH = 9, T = 25°C, I = 0.10 M, and λ_{ex} = 305 nm.

TD-DFT calculation

All density functional theory (DFT) and time-dependent density functional theory (TD-DFT) calculations were carried out using the Gaussian16W program[3] package at the b3lyp/6-31+G(d) level with applying the polarizable continuum model (PCM) to consider the solvent effect (water). The ground-state geometries were obtained by optimization calculation and confirmed the absence of imaginary frequencies by vibrational frequency calculation. All structure graphics and molecular orbitals were generated by GaussView6.[4]
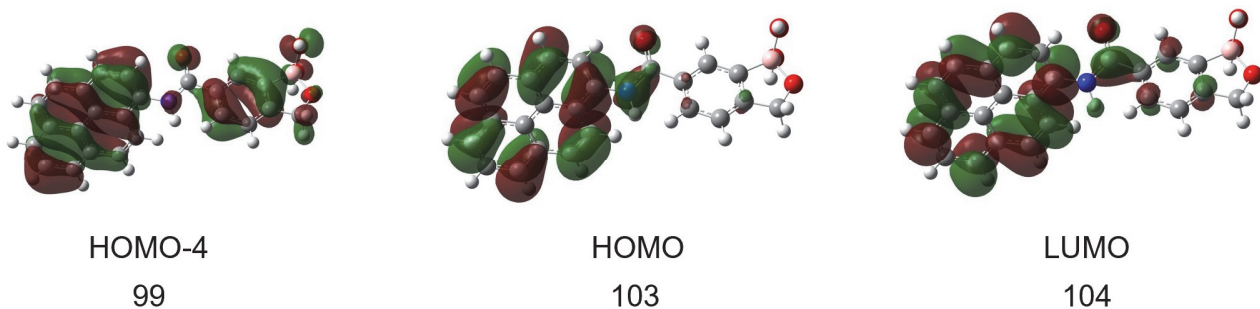

HOMO-4	HOMO	LUMO
99	103	104

Figure S4-1. Electron orbital maps for selected energy levels of *1*.

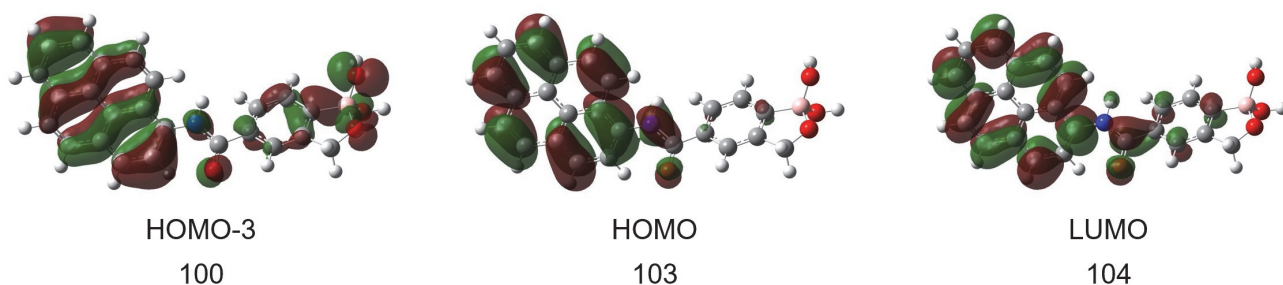| HOMO-3	HOMO	LUMO
100	103	104

Figure S4-2. Electron orbital maps for selected energy levels of *2*.

Table S1. Singlet electronic excitation energies together with composition and character based on the optimized ground state geometries of *1* and *2*.

|	Transition (OS) [a]	Energy / eV (nm)	State (Contribution)	Composition	Character
1	S_1 (0.7309)	3.27 (379)	103 → 104 (94.5%)	HOMO → LUMO	π-π* (pyrene)
	S_8 (0.2274)	4.31 (288)	99 → 104 (44.5%)	HOMO – 4 → LUMO	ICT (benzoxaborole→pyrene) [b] π-π* (pyrene)
2	S_1 (0.7363)	3.26 (380)	103 → 104 (94.6%)	HOMO → LUMO	π-π* (pyrene)
	S_7 (0.2086)	4.30 (289)	100 → 104 (50.0%)	HOMO – 3 → LUMO	ICT (benzoxaborole→pyrene) [b] π-π* (pyrene)

[a] OS means oscillator strength.

[b] ICT denotes intramolecular charge transfer.
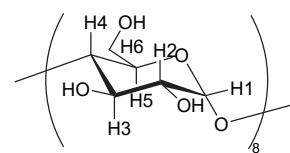
NOESY spectrum

(a)
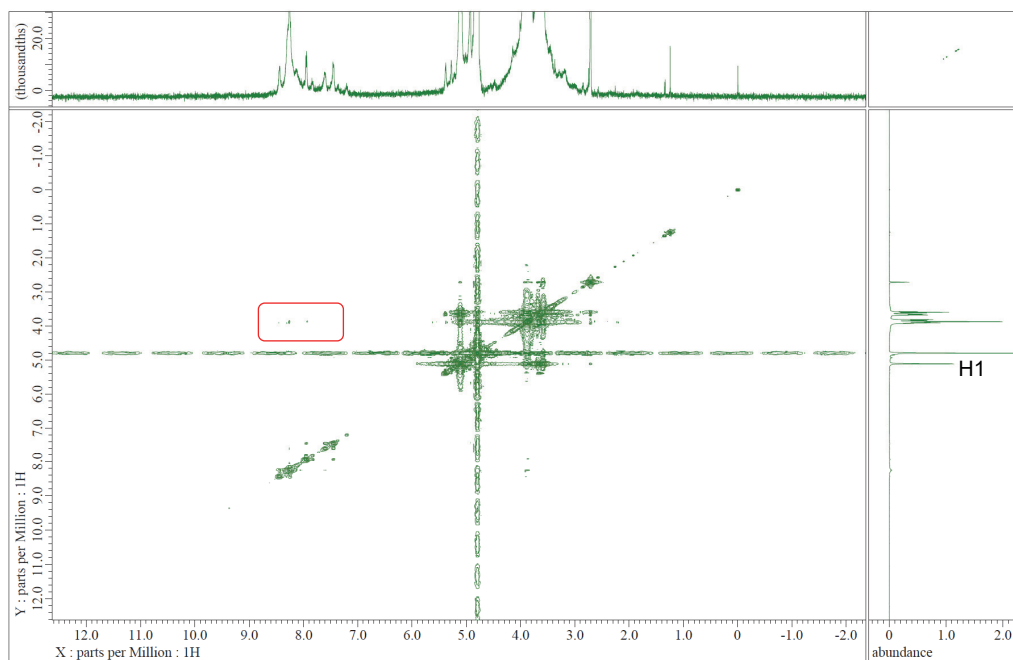
(b)
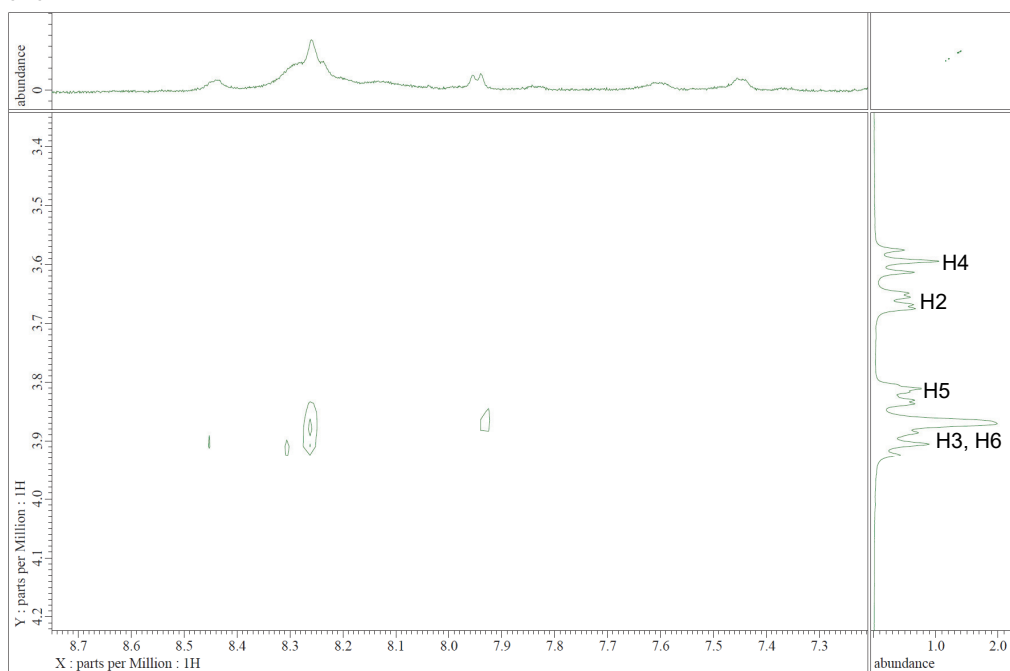
(c)

Figure S5. (a) NOESY spectrum of **1** with γ-CyD in a mixed solvent of 0.12 mL DMSO-d_6 and 0.48 mL D_2O (10 mM carbonate buffer, pD 10.6): C_{probe} = 2.22 mM, $C_{γCyD}$ = 10.4 mM, T = 23.8°C, 64 scans, acquisition time: 0.1364 sec, relaxation delay: 1.5 sec, mixing time: 0.2 seconds. (b) Enlarged spectrum of Fig. S5a. (c) The structure of γ-CyD.[5]
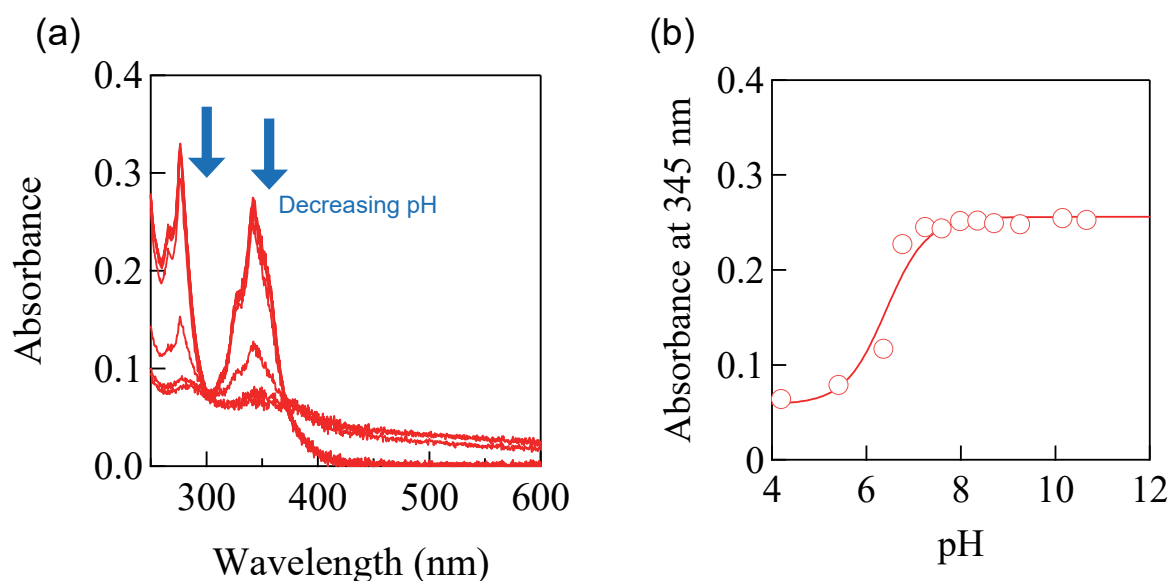
pH dependence of UV-vis absorption spectra

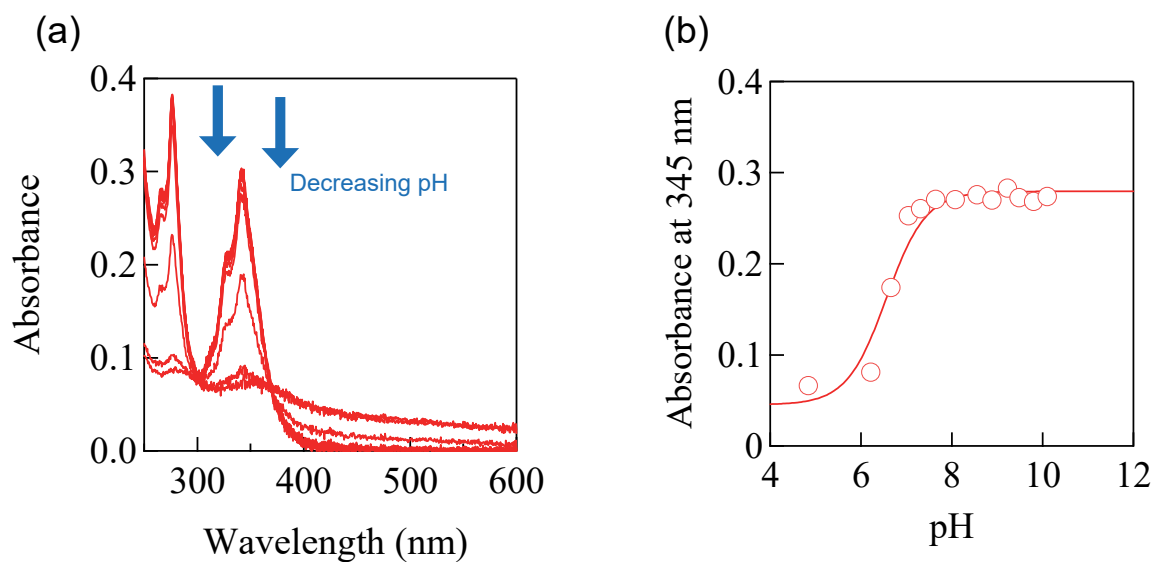Figure S6-1. (a) UV-vis absorption spectra of **1/γCyD** under various pH conditions and (b) change in absorbance at 345 nm in DMSO/water (2/98 in v/v): C_{probe} = 10.3 μM, $C_{\gamma CyD}$ = 5 mM, 10 mM of phosphate buffer, T = 25°C, and I = 0.10 M.

Figure S6-2. (a) UV-vis absorption spectra of **2/γCyD** under various pH conditions and (b) change in absorbance at 345 nm in DMSO/water (2/98 in v/v): C_{probe} = 11.3 μM, $C_{\gamma CyD}$ = 5 mM, 10 mM of phosphate buffer, T = 25°C, and I = 0.10 M.
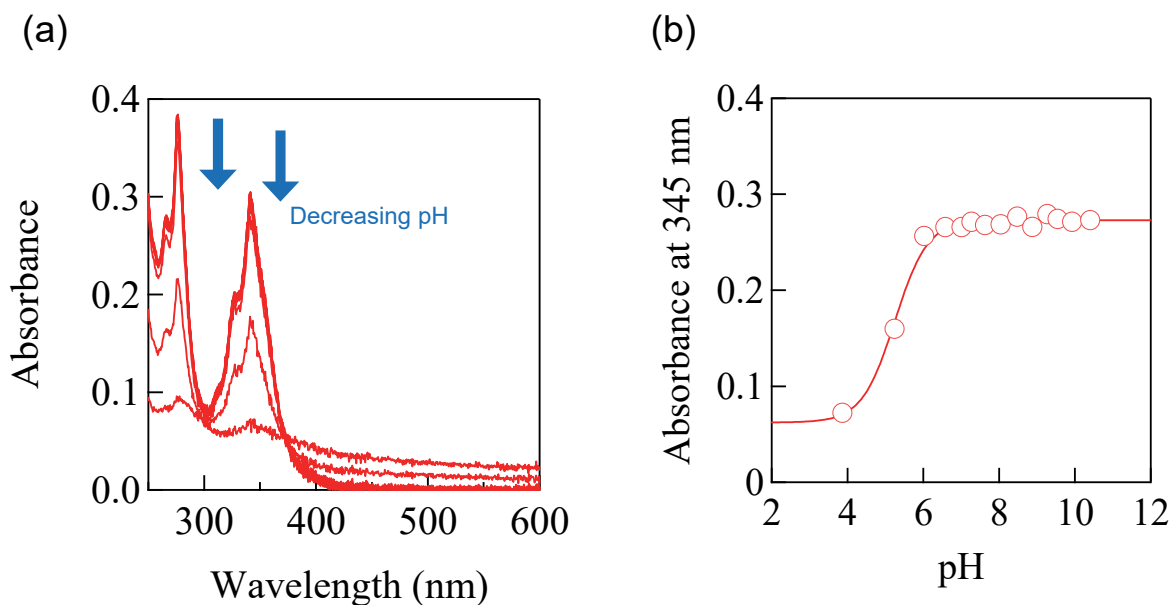
Figure S7-1. (a) UV-vis absorption spectra of *1/γCyD* under various pH conditions and (b) change in absorbance at 345 nm in the presence of D-fructose (30.0 mM) in DMSO/water (2/98 in v/v): C_{probe} = 10.3 μM, $C_{\gamma CyD}$ = 5 mM, 10 mM of phosphate buffer, T = 25°C, and I = 0.10 M.
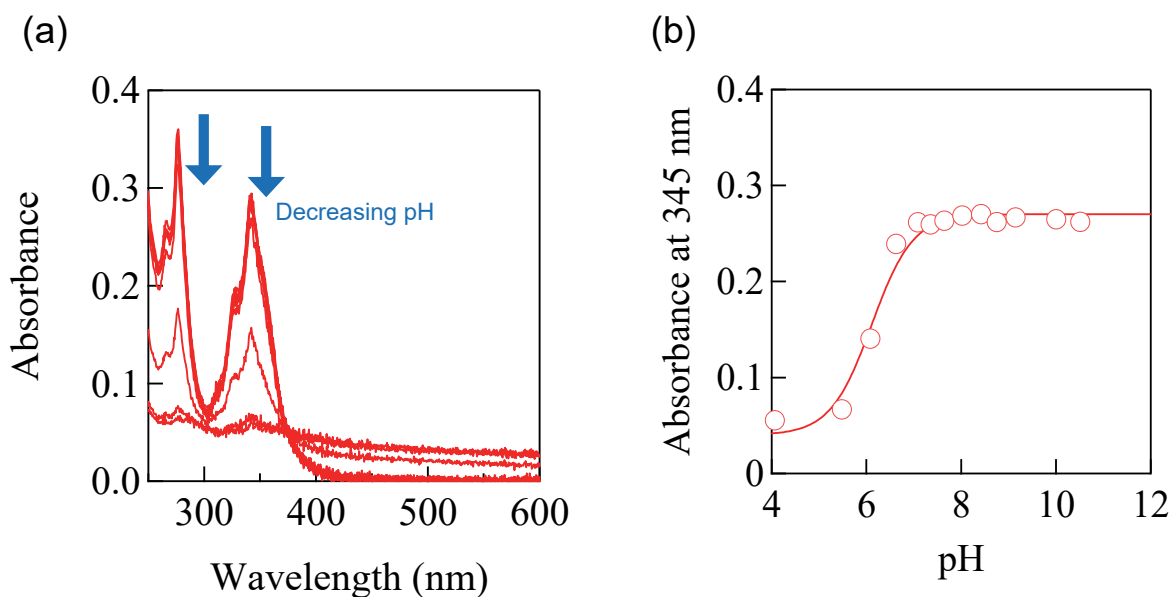

Figure S7-2. (a) UV-vis absorption spectra of *1/γCyD* under various pH conditions and (b) change in absorbance at 345 nm in the presence of D-glucose (29.7 mM) in DMSO/water (2/98 in v/v): C_{probe} = 10.3 μM, $C_{\gamma CyD}$ = 5 mM, 10 mM of phosphate buffer, T = 25°C, and I = 0.10 M.
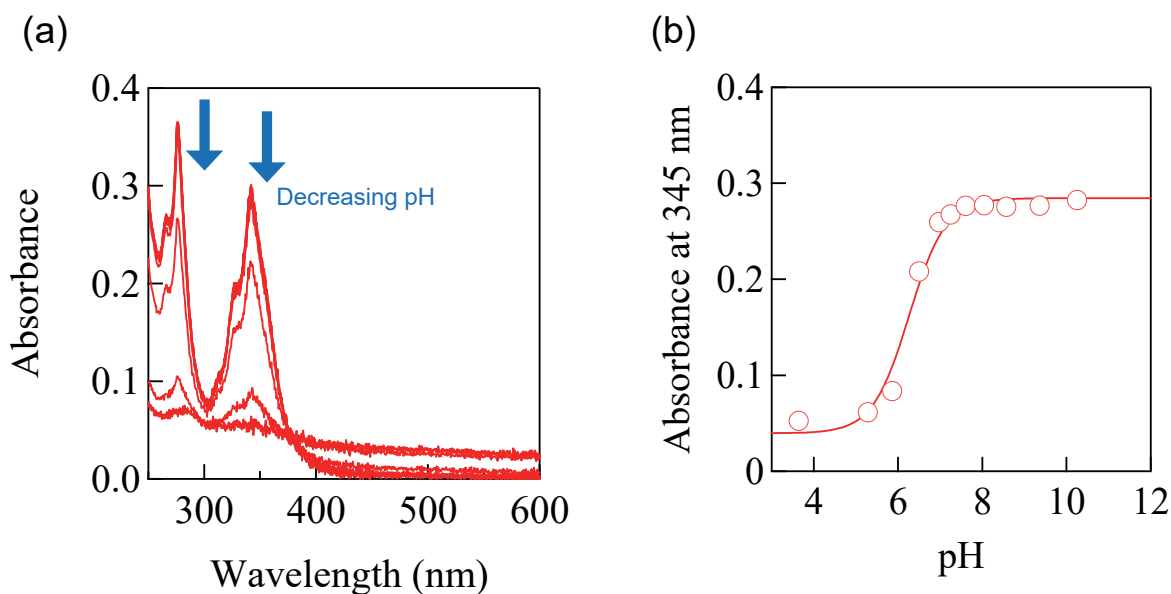
S11

Figure S7-3. (a) UV-vis absorption spectra of **1/γCyD** under various pH conditions and (b) change in absorbance at 345 nm in the presence of D-galactose (30.0 mM) in DMSO/water (2/98 in v/v): C_{probe} = 10.3 μM, $C_{γCyD}$ = 5 mM, 10 mM of phosphate buffer, T = 25°C, and I = 0.10 M.
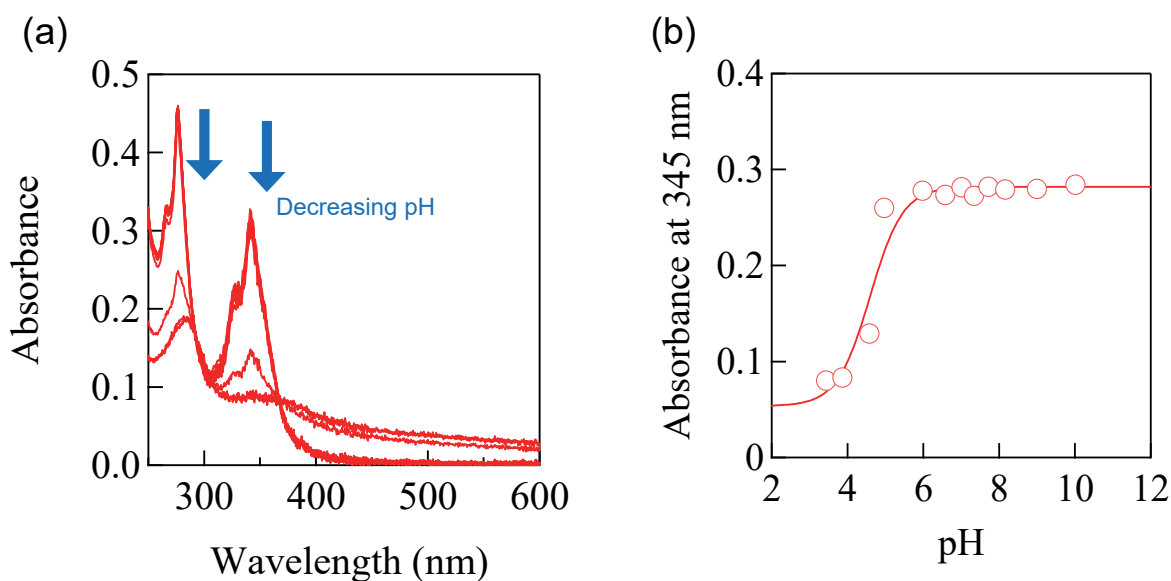

Figure S7-4. (a) UV-vis absorption spectra of **1/γCyD** under various pH conditions and (b) change in absorbance at 345 nm in the presence of D-allulose (31.1 mM) in DMSO/water (2/98 in v/v): C_{probe} = 10.3 μM, $C_{γCyD}$ = 5 mM, 10 mM of phosphate buffer, T = 25°C, and I = 0.10 M.

S12

Figure S7-5. (a) UV-vis absorption spectra of **2/γCyD** under various pH conditions and (b) change in absorbance at 345 nm in the presence of D-fructose (30.0 mM) in DMSO/water (2/98 in v/v): C_{probe} = 11.3 μM, $C_{γCyD}$ = 5 mM, 10 mM of phosphate buffer, T = 25°C, and I = 0.10 M.
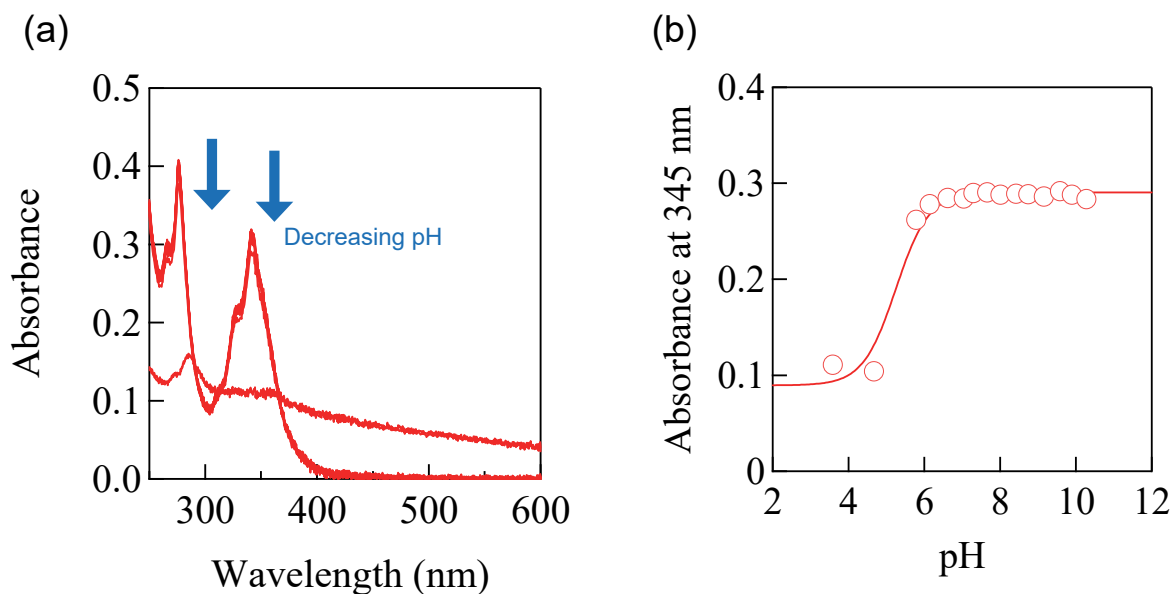

Figure S7-6. (a) UV-vis absorption spectra of **2/γCyD** under various pH conditions and (b) change in absorbance at 345 nm in the presence of D-glucose (29.7 mM) in DMSO/water (2/98 in v/v): C_{probe} = 11.3 μM, $C_{γCyD}$ = 5 mM, 10 mM of phosphate buffer, T = 25°C, and I = 0.10 M.
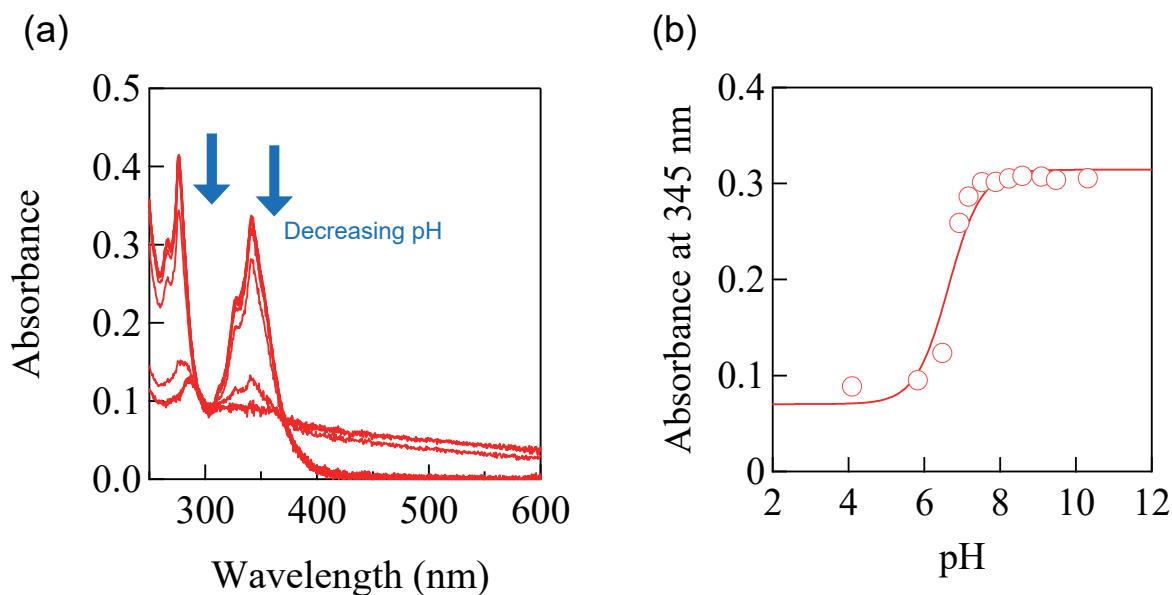
Figure S7-7. (a) UV-vis absorption spectra of **2/γCyD** under various pH conditions and (b) change in absorbance at 345 nm in the presence of D-galactose (30.0 mM) in DMSO/water (2/98 in v/v): C_{probe} = 11.3 μM, $C_{γCyD}$ = 5 mM, 10 mM of phosphate buffer, T = 25°C, and I = 0.10 M.
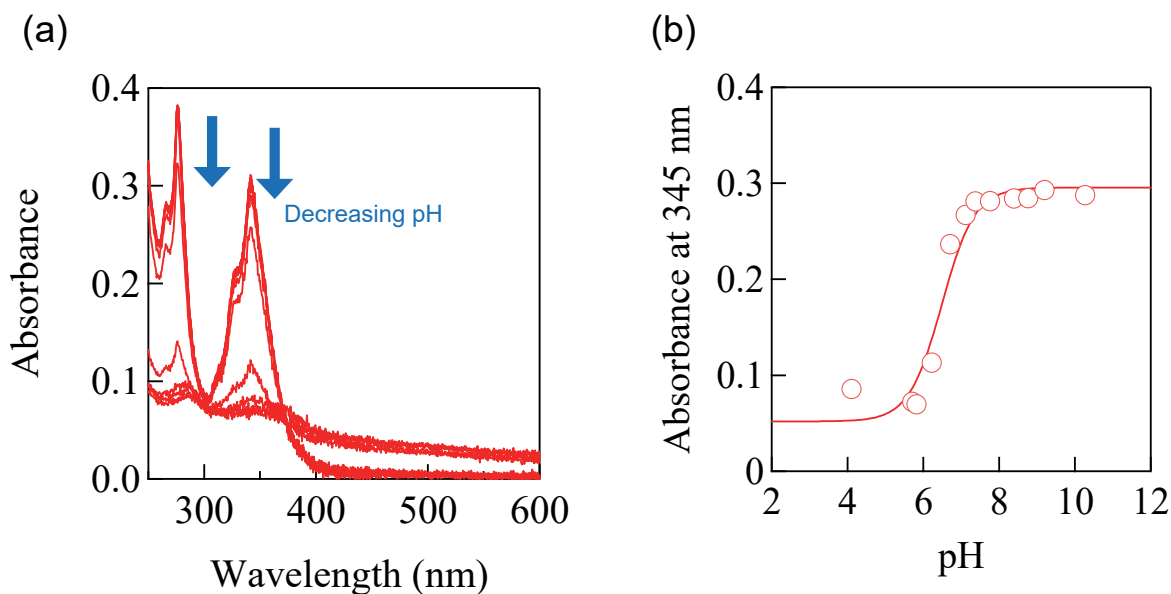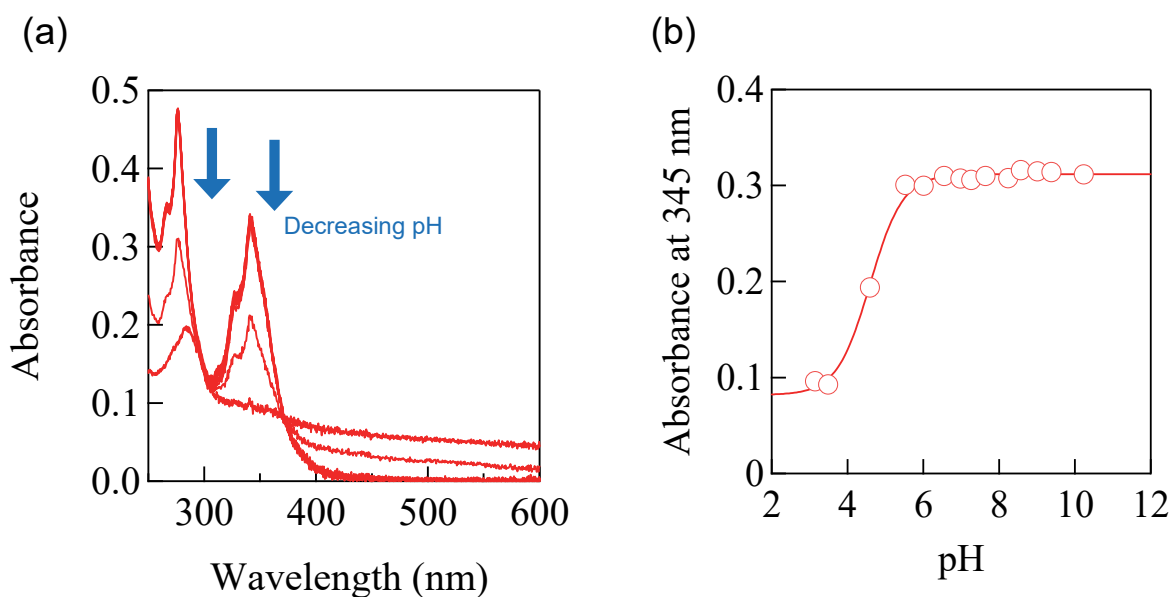

Figure S7-8. (a) UV-vis absorption spectra of **2/γCyD** under various pH conditions and (b) change in absorbance at 345 nm in the presence of D-allulose (26.3 mM) in DMSO/water (2/98 in v/v): C_{probe} = 11.3 μM, $C_{γCyD}$ = 5 mM, 10 mM of phosphate buffer, T = 25°C, and I = 0.10 M.

Table S2. Apparent acid dissociation constants of **1/γCyD** and **2/γCyD** in the absence and presence of saccharides.[a]

	1	*2*
Probe	6.41 ± 0.14	6.56 ± 0.12
Probe + D-fructose	5.25 ± 0.06	5.25 ± 0.12
Probe + D-glucose	6.11 ± 0.09	6.64 ± 0.14
Probe + D-galactose	6.26 ± 0.09	6.49 ± 0.15
Probe + D-allulose	4.60 ± 0.16	4.59 ± 0.05

[a] In DMSO/water (2/98 in v/v) at $T = 25°C$ and $I = 0.10$ M in the presence of 10 mM phosphate buffer.
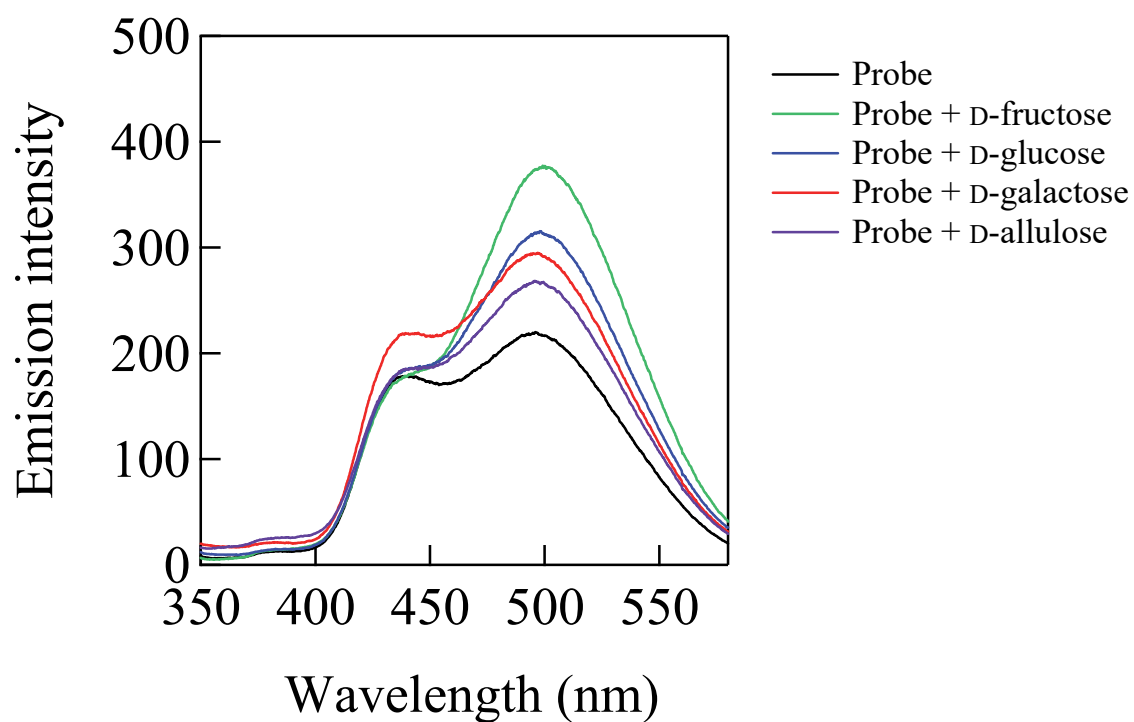
Fluorescence response of *2/γCyD* to saccharides

Figure S8. Fluorescence spectra of *2/γCyD* in the absence (black) and presence of each saccharide (30 mM) in DMSO/water (2/98 in v/v): C_{probe} = 9.99 μM, $C_{γCyD}$ = 5 mM, 10 mM of phosphate buffer, pH = 7.4, T = 25°C, I = 0.10 M, and λ_{ex} = 305 nm.

pH dependence of fluorescence spectra

Figure S9-1. Fluorescence spectra of *1/γCyD* under various pH conditions in the absence (a) and presence of 30 mM D-fructose (b), D-glucose (c), D-galactose (d) and D-allulose (e) in DMSO/water (2/98 in v/v): C_{probe} = 10.3 μM, $C_{γCyD}$ = 5 mM, 10 mM of phosphate buffer, T = 25°C, I = 0.10 M, and $λ_{ex}$ = 305 nm.
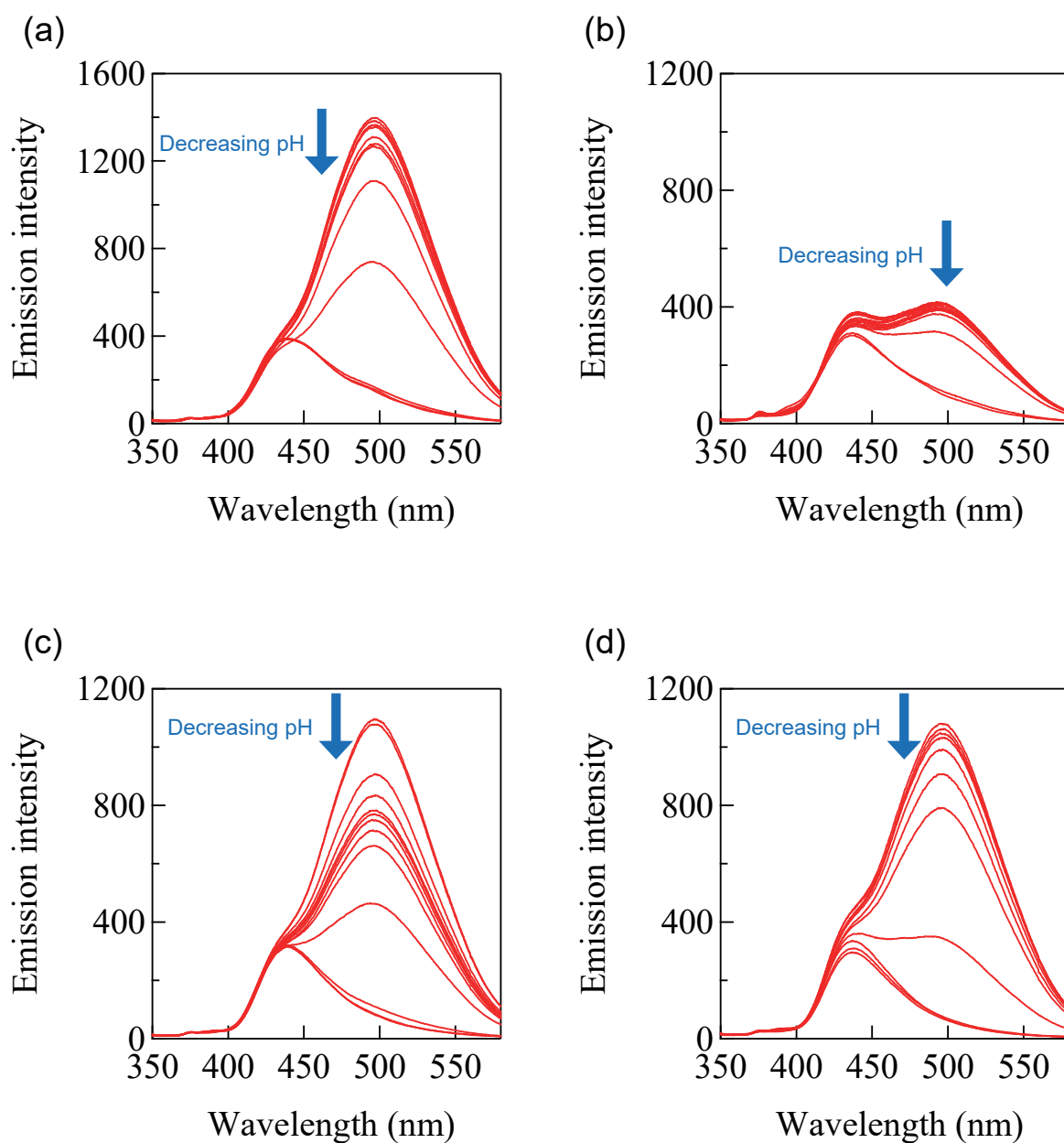
(e)

Figure S9-1. Fluorescence spectra of **1/γCyD** under various pH conditions in the absence (a) and presence of 30 mM D-fructose (b), D-glucose (c), D-galactose (d) and D-allulose (e) in DMSO/water (2/98 in v/v): C_{probe} = 10.3 μM, $C_{\gamma CyD}$ = 5 mM, 10 mM of phosphate buffer, T = 25°C, I = 0.10 M, and λ_{ex} = 305 nm. (Continued)
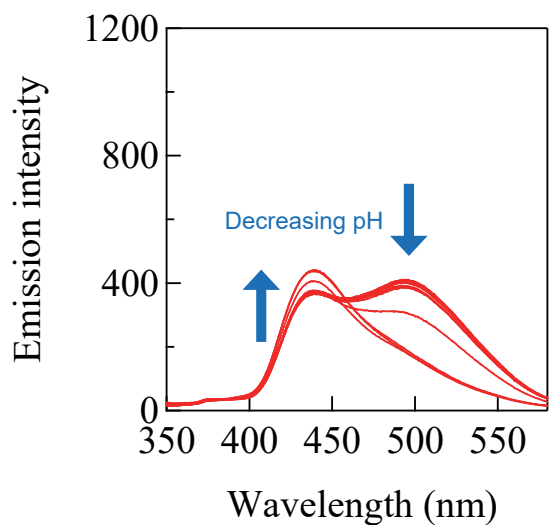
Figure S9-2. Fluorescence spectra of **2/γCyD** under various pH conditions in the absence (a) and presence of 30 mM D-fructose (b), D-glucose (c), D-galactose (d) and D-allulose (e) in DMSO/water (2/98 in v/v): C_{probe} = 11.3 μM, $C_{γCyD}$ = 5 mM, 10 mM of phosphate buffer, T = 25°C, I = 0.10 M, and $λ_{ex}$ = 305 nm.
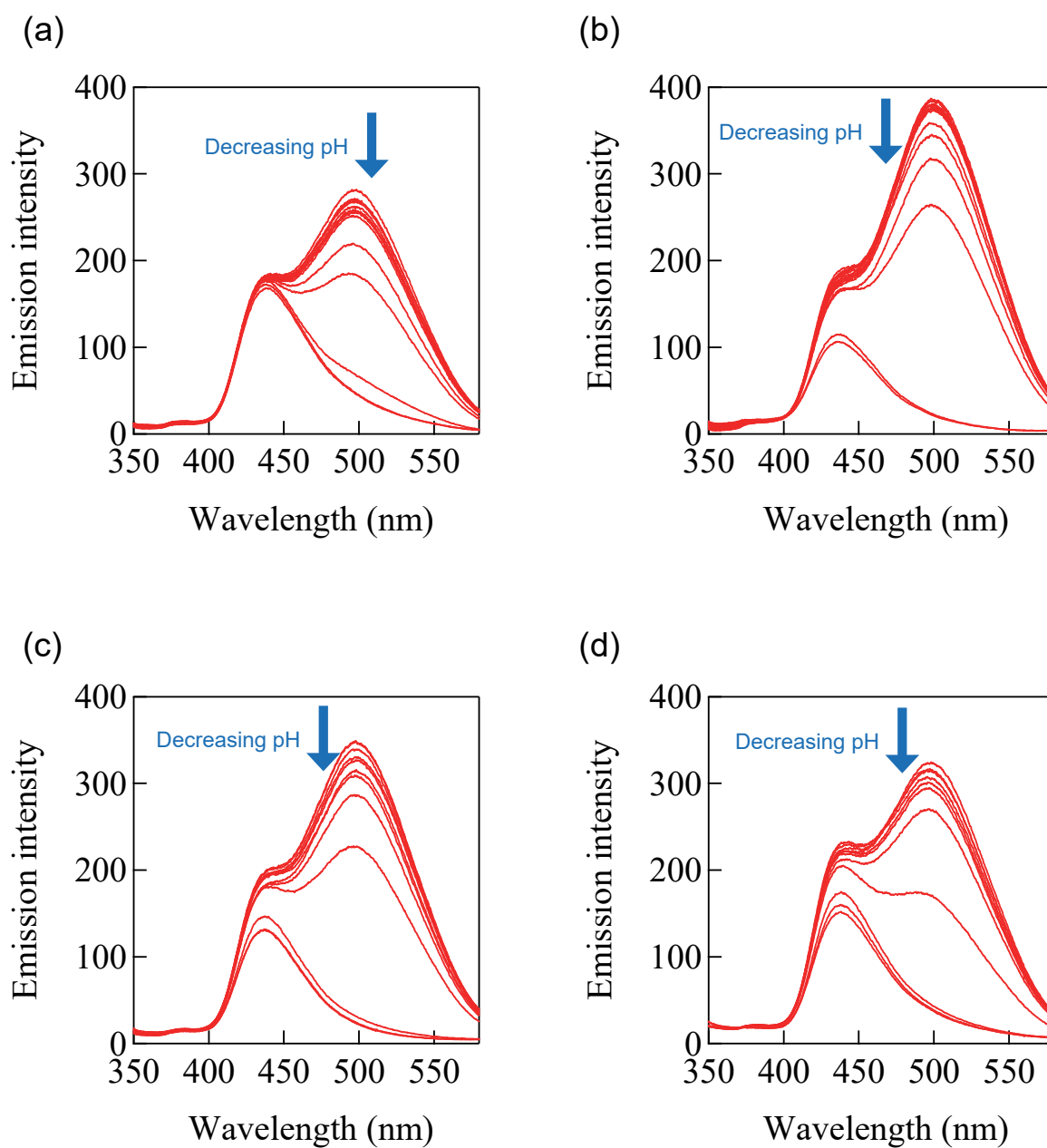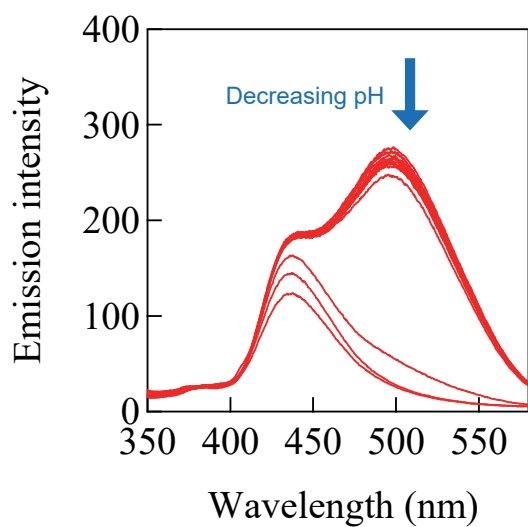
(e)

Figure S9-2. Fluorescence spectra of **2/γCyD** under various pH conditions in the absence (a) and presence of 30 mM D-fructose (b), D-glucose (c), D-galactose (d) and D-allulose (e) in DMSO/water (2/98 in v/v): C_{probe} = 11.3 µM, $C_{\gamma CyD}$ = 5 mM, 10 mM of phosphate buffer, T = 25°C, I = 0.10 M, and λ_{ex} = 305 nm. (Continued)

Figure S10-1. Ratio of fluorescence intensities at 500 and 430 nm (I_{500}/I_{430}) of **1/γCyD** under various pH conditions in the absence and presence of each saccharide (30 mM) in DMSO/water (2/98 in v/v) in Figure S9-1.
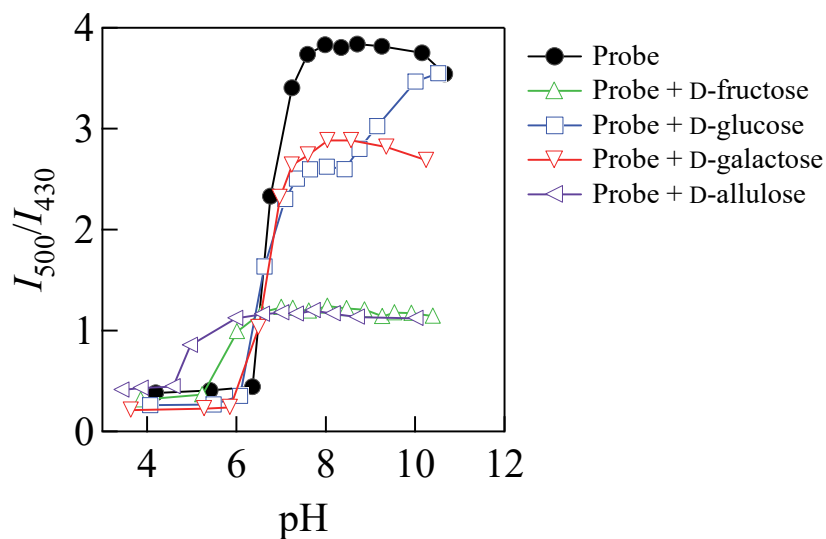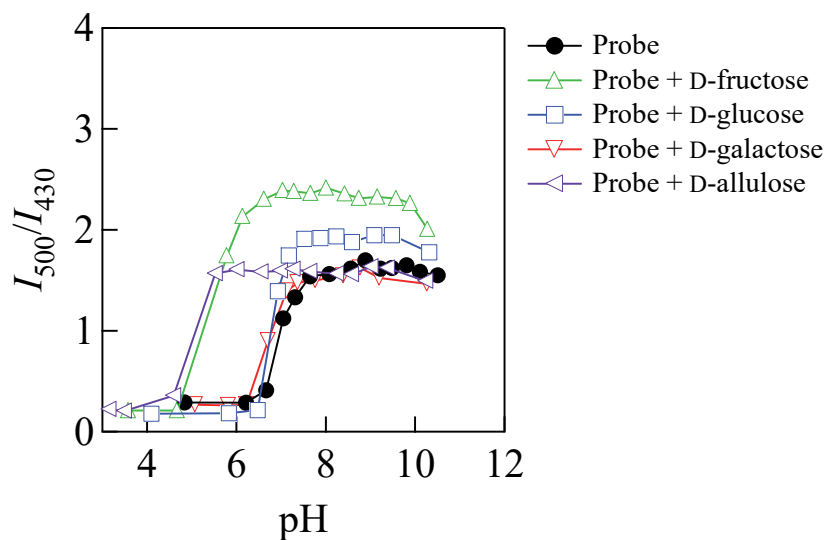

Figure S10-2. Ratio of fluorescence intensities at 500 and 430 nm (I_{500}/I_{430}) of **2/γCyD** under various pH conditions in the absence and presence of each saccharide (30 mM) in DMSO/water (2/98 in v/v) in Figure S9-2.
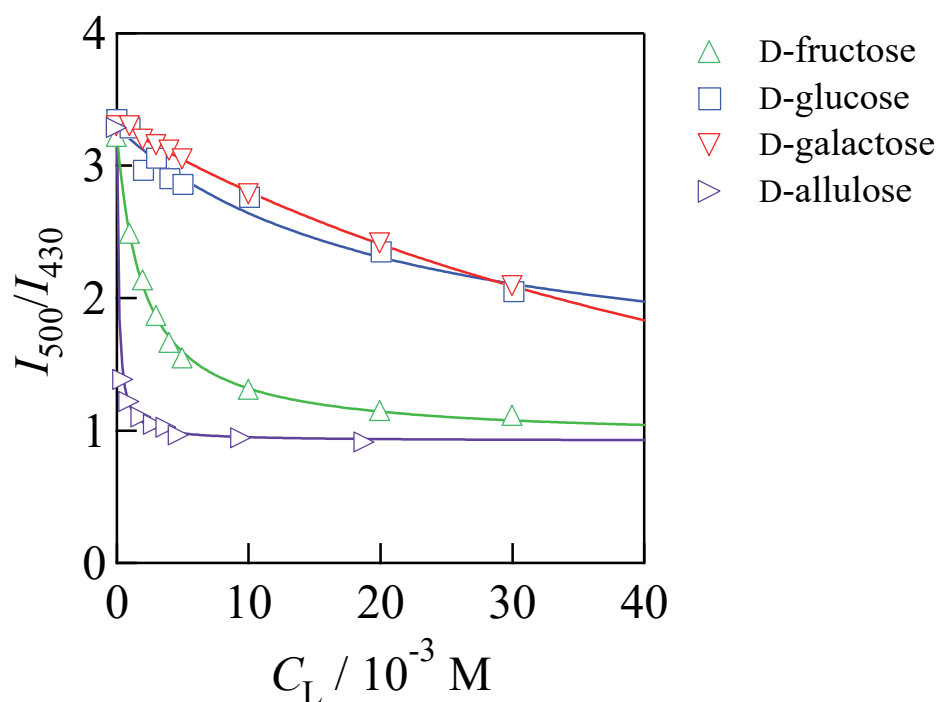
Figure S11-1. Ratio of fluorescence intensities at 500 and 430 nm (I_{500}/I_{430}) of *1/γCyD* at various concentrations of each saccharide in DMSO/water (2/98 in v/v): C_{probe} = 10.7 µM, $C_{γCyD}$ = 5 mM, 10 mM of phosphate buffer, pH = 7.4, T = 25°C, I = 0.10 M, and $λ_{ex}$ = 305 nm. Each solid curve indicates a theoretical curve derived from the 1:1 binding model fitted by non-linear least squares analysis for each reaction system.

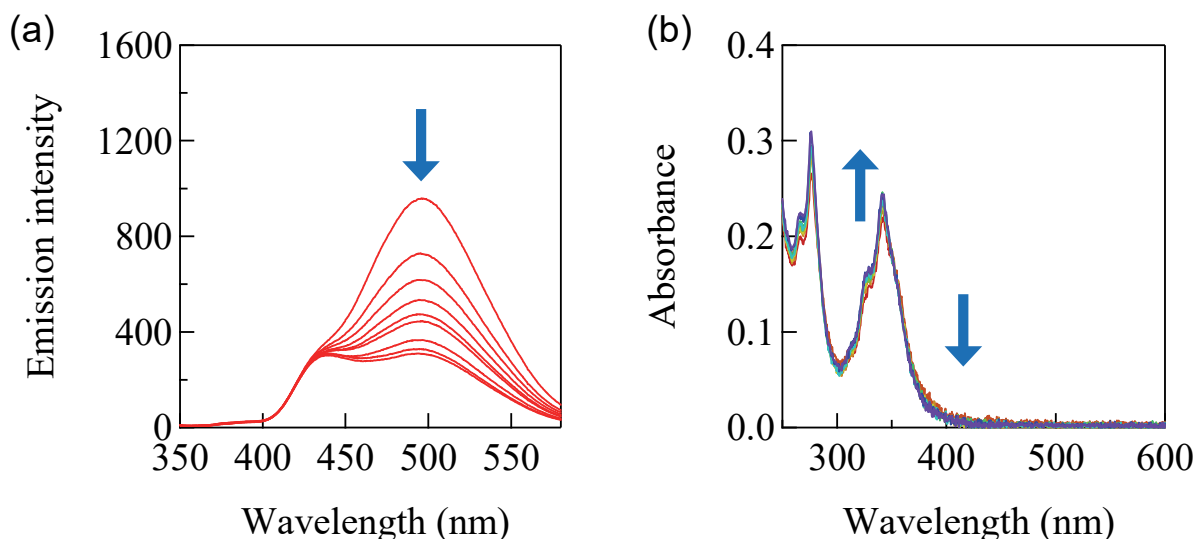Figure S11-2. Fluorescence (a) and UV-vis absorption (b) spectra of **1/γCyD** at various concentrations of D-fructose (0, 1.00, 2.00, 3.00, 4.00, 5.00, 10.0, 20.0, 30.0 mM) in DMSO/water (2/98 in v/v): C_{probe} = 10.7 μM, $C_{\gamma CyD}$ = 5 mM, 10 mM of phosphate buffer, pH = 7.4, T = 25°C, I = 0.10 M, and λ_{ex} = 305 nm for (a).
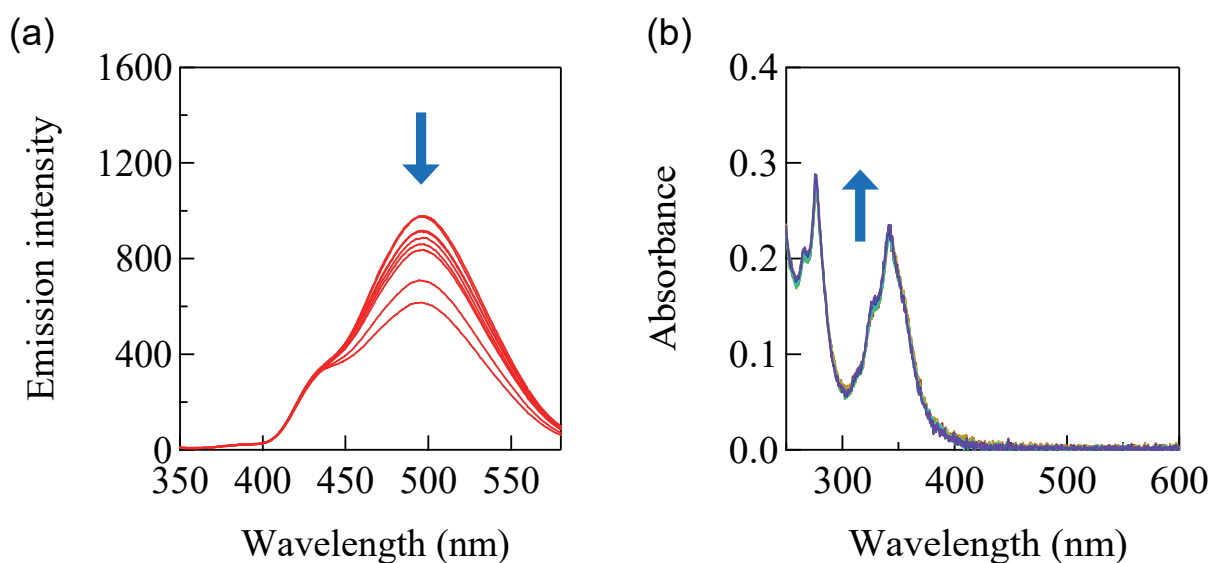

Figure S11-3. Fluorescence (a) and UV-vis absorption (b) spectra of **1/γCyD** at various concentrations of D-glucose (0, 1.01, 2.00, 3.01, 4.02, 5.01, 10.1, 20.0, 30.1 mM) in DMSO/water (2/98 in v/v): C_{probe} = 10.7 μM, $C_{\gamma CyD}$ = 5 mM, 10 mM of phosphate buffer, pH = 7.4, T = 25°C, I = 0.10 M, and λ_{ex} = 305 nm for (a).
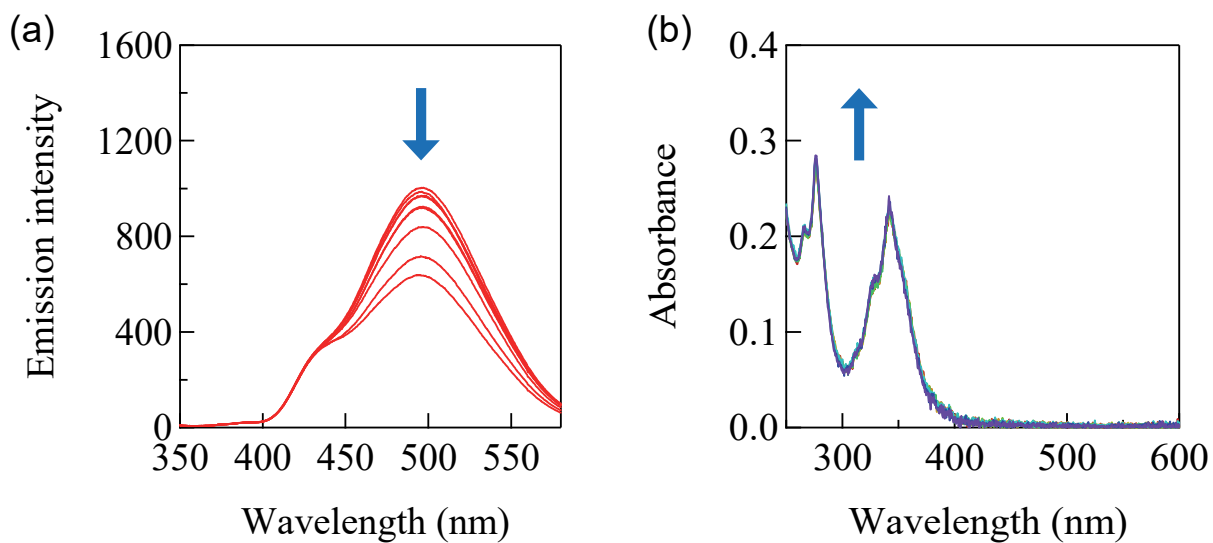
Figure S11-4. Fluorescence (a) and UV-vis absorption (b) spectra of *1/γCyD* at various concentrations of D-galactose (0, 1.00, 2.00, 3.00, 4.00, 5.00, 10.0, 20.0, 30.0 mM) in DMSO/water (2/98 in v/v): C_{probe} = 10.7 μM, $C_{γCyD}$ = 5 mM, 10 mM of phosphate buffer, pH = 7.4, T = 25°C, I = 0.10 M, and $λ_{ex}$ = 305 nm for (a).
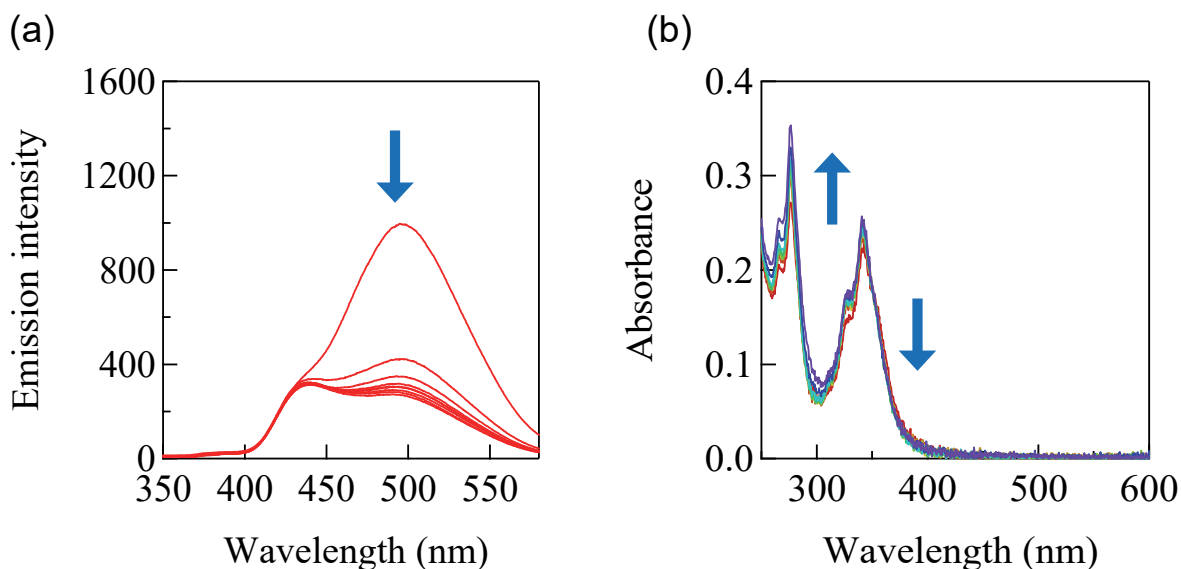

Figure S11-5. Fluorescence (a) and UV-vis absorption (b) spectra of *1/γCyD* at various concentrations of D-allulose (0, 0.474, 0.942, 1.88, 2.82, 3.76, 4.70, 9.42, 18.8, 28.2 mM) in DMSO/water (2/98 in v/v): C_{probe} = 10.7 μM, $C_{γCyD}$ = 5 mM, 10 mM of phosphate buffer, pH = 7.4, T = 25°C, I = 0.10 M, and $λ_{ex}$ = 305 nm for (a).

Competition experiment
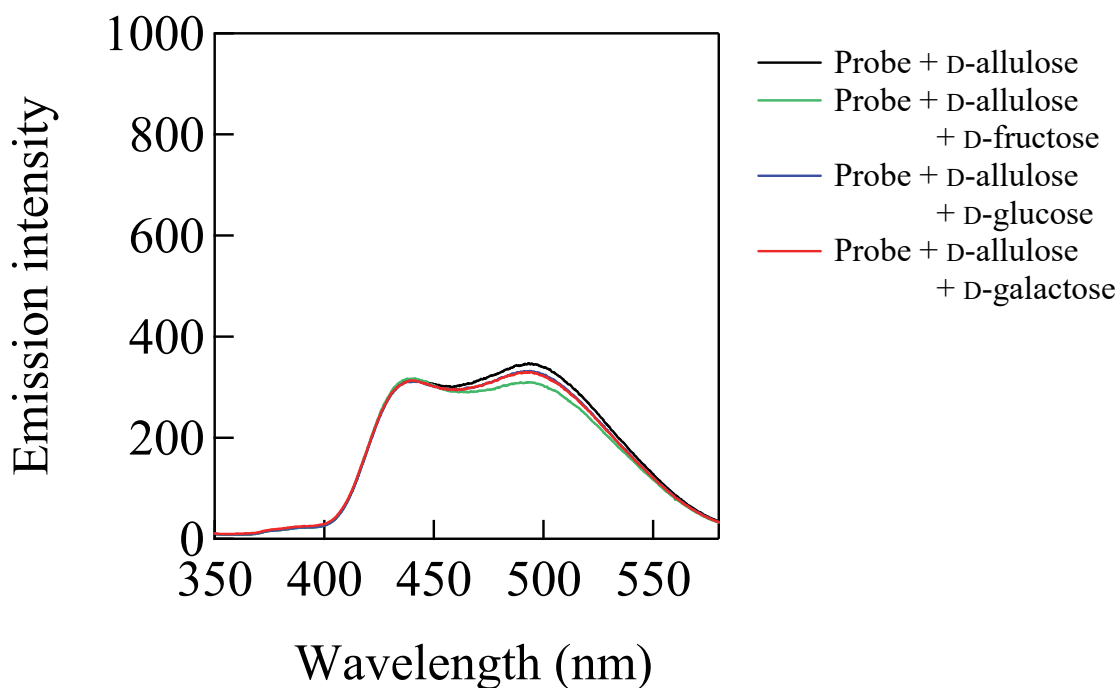
Figure S12-1. Fluorescence spectra of **1/γCyD** with D-allulose (1.01 mM) in the absence and presence of saccharides (1 mM) in DMSO/water (2/98 in v/v): C_{probe} = 10.7 µM, $C_{\gamma CyD}$ = 5 mM, 10 mM of phosphate buffer, pH = 7.4, T = 25°C, I = 0.10 M, and λ_{ex} = 305 nm.

a: Probe
b: Probe + D-fructose
c: Probe + D-glucose
d: Probe + D-galactose
e: Probe + D-allulose
f: Probe + D-allulose
            + D-fructose
g: Probe + D-allulose
            + D-glucose
h: Probe + D-allulose
            + D-galactose

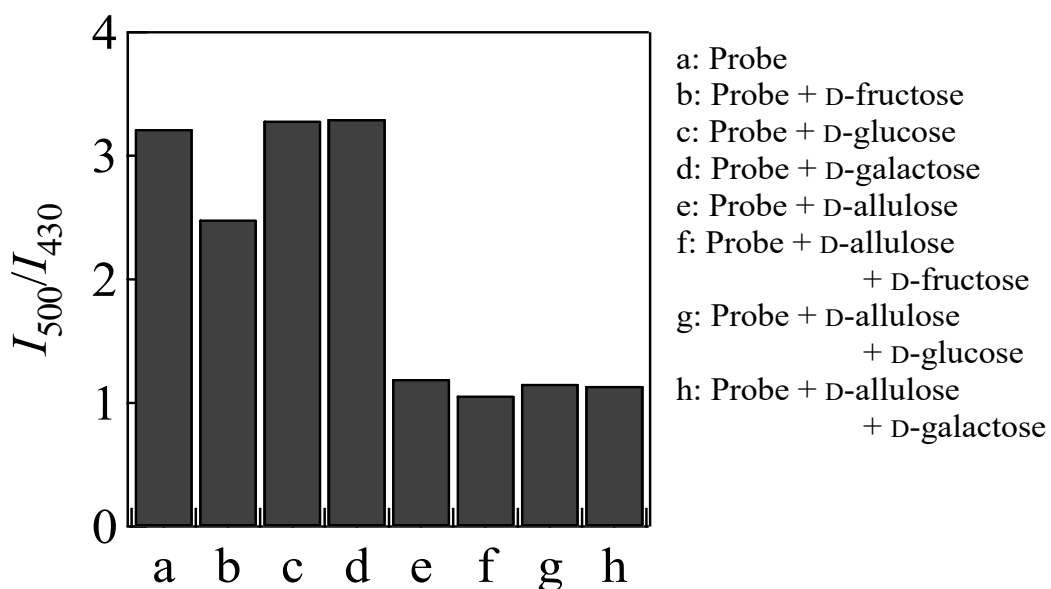Figure S12-2. Ratio of fluorescence intensities at 500 and 430 nm (I_{500}/I_{430}) of **1/γCyD** in the absence and presence of saccharides (1 mM) in DMSO/water (2/98 in v/v) in Figures 1 and S12-1.
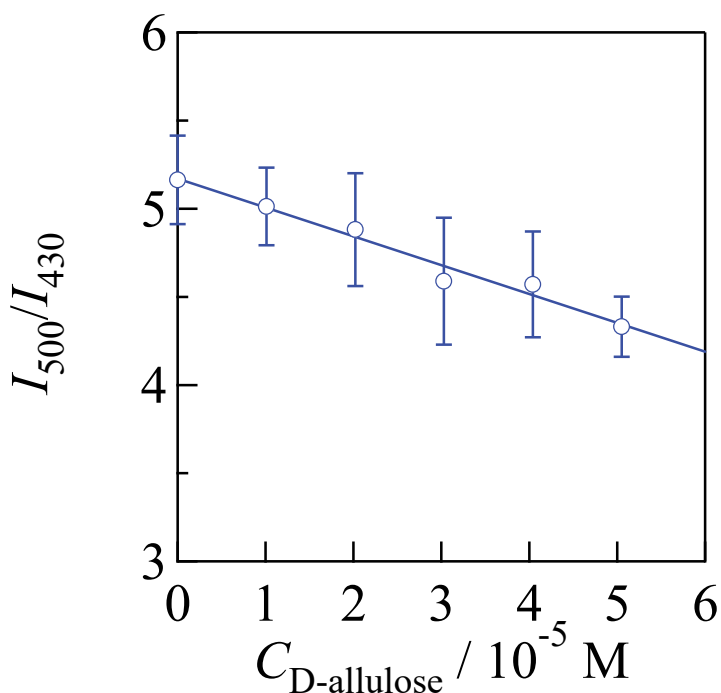
Limits of detection and quantification

Figure S13. Calibration curve of *1/γCyD* for the quantification of D-allulose: C_{probe} = 11.3 µM, $C_{\gamma CyD}$ = 5 mM, 10 mM of phosphate buffer, pH = 8.0, T = 25°C, I = 0.10 M, and λ_{ex} = 305 nm.

The limit of detection (LOD) and limit of quantification (LOQ) of *1/γCyD* were calculated as following equations.

$$\mathrm{LOD} = -\frac{3.3\sigma}{a} \tag{S1}$$

$$\mathrm{LOQ} = -\frac{10\sigma}{a} \tag{S2}$$

In these equations, a is a slope of calibration curve. σ denotes the standard deviation of blank data, that is, fluorescence intensity of *1/γCyD* in the absence of D-allulose. The σ value was calculated according to eqn (S3).

$$\sigma = \sqrt{\frac{\sum_{i=1}^{n}(R_{B,i} - R_{B,ave})^2}{n-1}} \tag{S3}$$

where $R_{B,i}$, $R_{B,ave}$ and n represent I_{500}/I_{430} of each blank measurement, the average of $R_{B,i}$ and the number of repeated measurements (n = 10), respectively. The σ value was determined to be 0.034.

Tautomeric forms of D-fructose and D-allulose in aqueous solution

β-D-fructofuranose
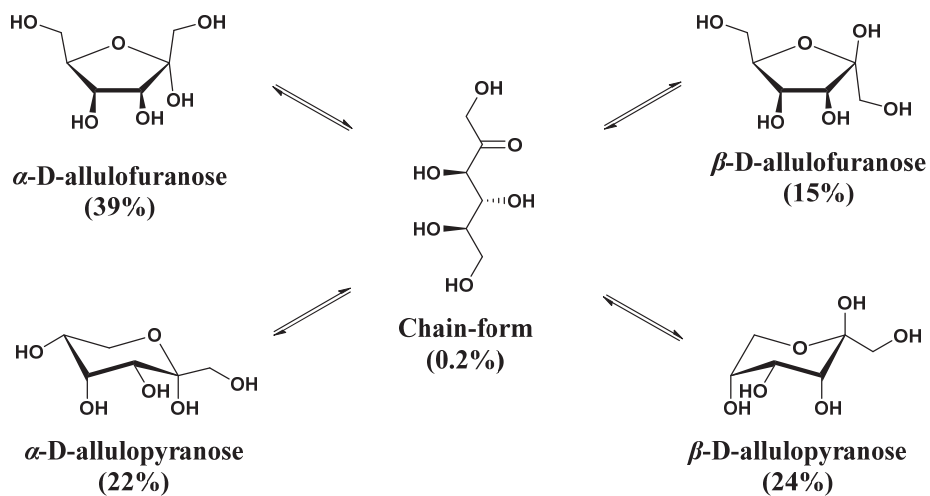**(22.35%)**

Chain-form
(0.50%)

α-D-fructofuranose
(6.24%)

β-D-fructopyranose
(68.23%)

α-D-fructopyranose
(2.67%)
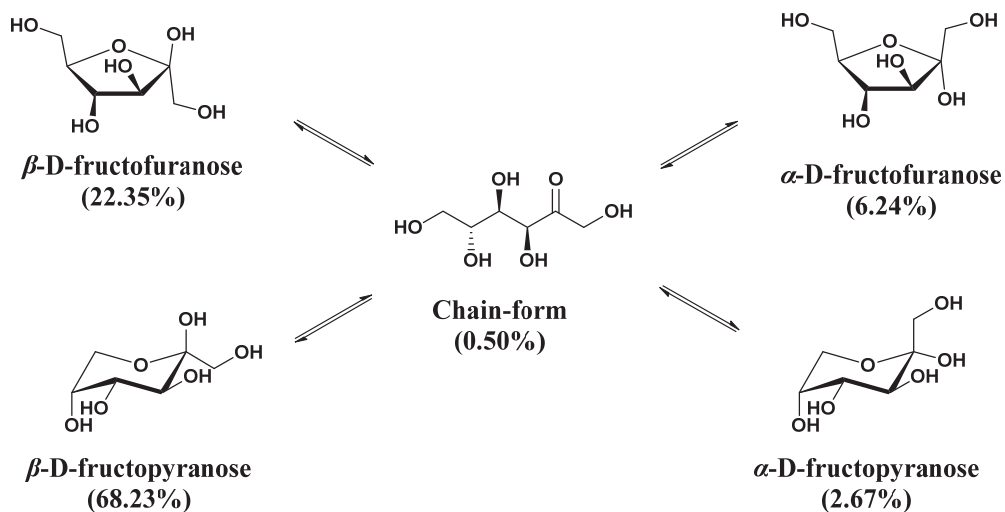
Scheme S2-1. Tautomeric forms of D-fructose in aqueous solution.[6]

α-D-allulofuranose
(39%)

Chain-form
(0.2%)

β-D-allulofuranose
(15%)

α-D-allulopyranose
(22%)

β-D-allulopyranose
(24%)

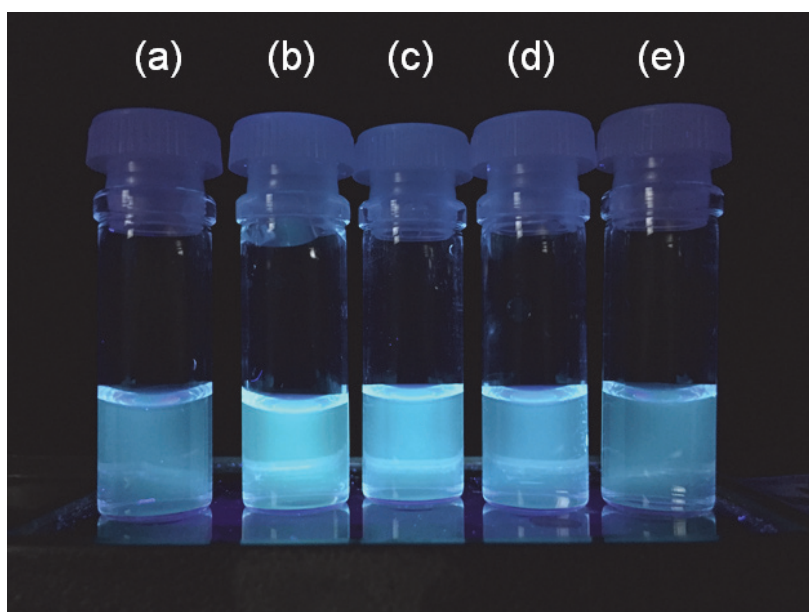Scheme S2-2. Tautomeric forms of D-allulose in aqueous solution.[7]

Figure S14. Photograph of the fluorescence of **2/γCyD** in the absence (a) and presence of 1 mM of D-fructose (b), D-glucose (c) D-galactose (d) and D-allulose (e) in DMSO/water (2/98 in v/v) at room temperature with 365 nm UV light: C_{probe} = 11.3 µM, $C_{γCyD}$ = 5 mM, 10 mM of phosphate buffer, pH = 7.4, and I = 0.10 M.

CD spectrum of D-allulose

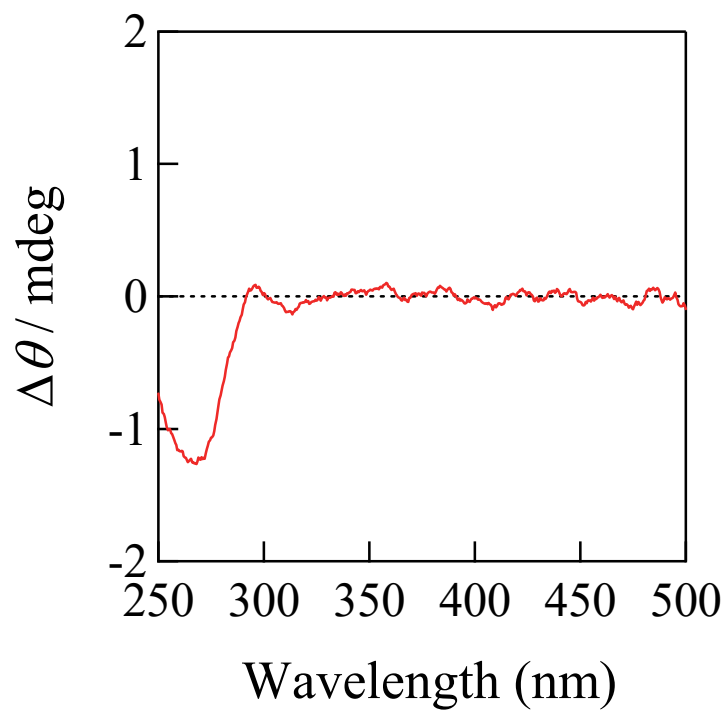
Figure S15. Circular dichroism spectrum of D-allulose (9.58 mM) in water: 10 mM of phosphate buffer, pH = 7.4, and T = 25°C.

ICD and UV-vis absorption spectra

Figure S16-1. UV-vis absorption spectra of *1/γCyD* in the absence and presence of each saccharide (10 mM) in DMSO/water (2/98 in v/v): C_{probe} = 10.3 µM, $C_{γCyD}$ = 5 mM, 10 mM of phosphate buffer, pH = 10.2, T = 25°C, and I = 0.10 M.

Figure S16-2. ICD spectra of *2/γCyD* in the absence and presence of each saccharide (10 mM) in DMSO/water (2/98 in v/v): C_{probe} = 9.99 µM, $C_{γCyD}$ = 5 mM, 10 mM of phosphate buffer, pH = 10.2, T = 25°C, and I = 0.10 M.

S30
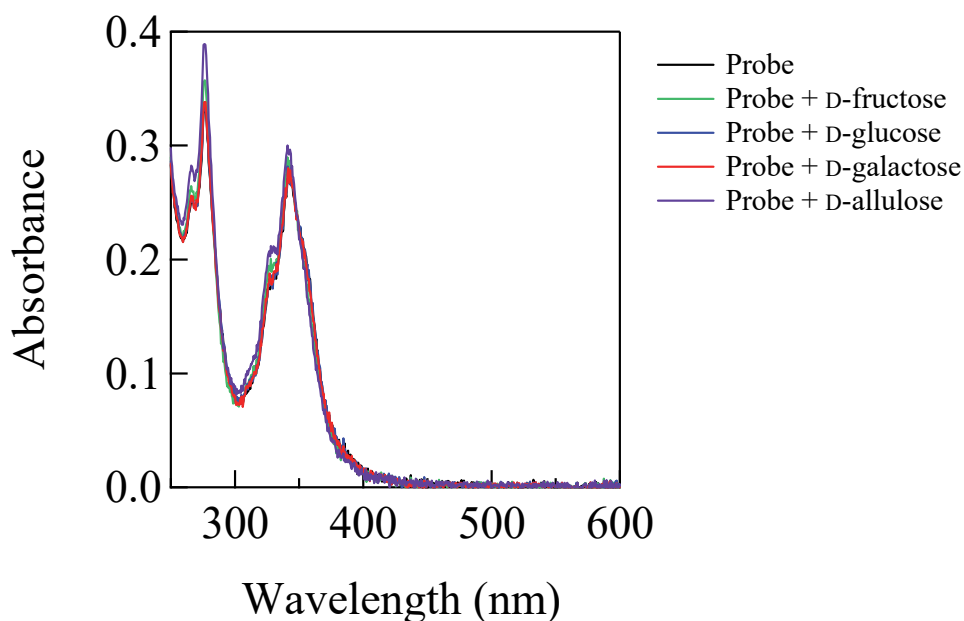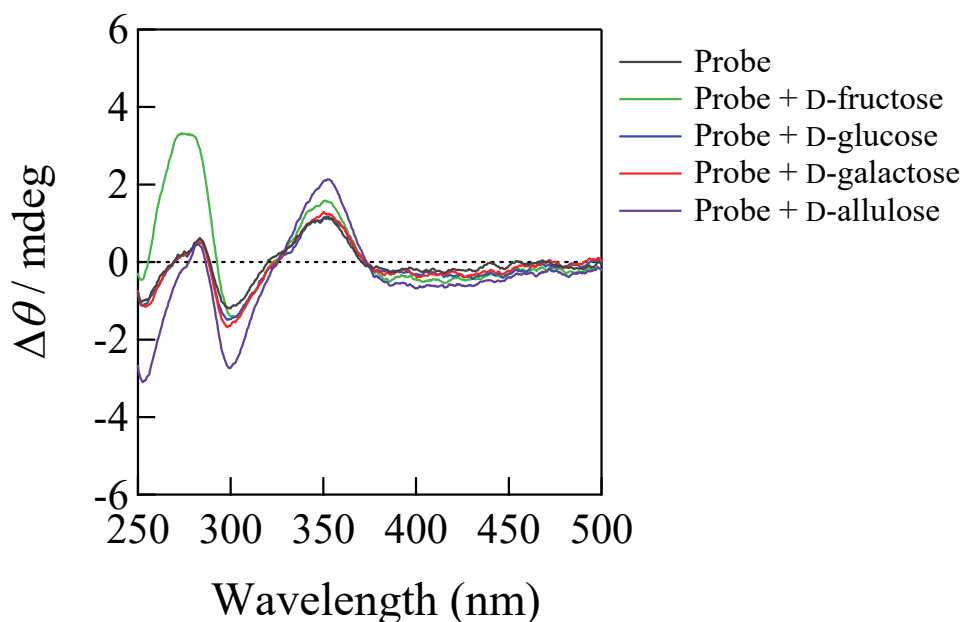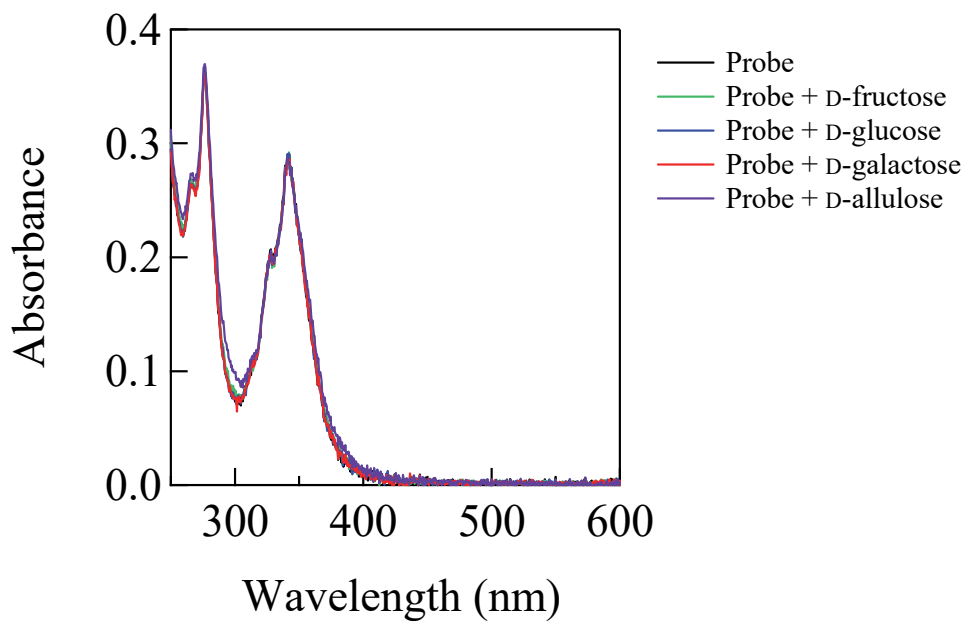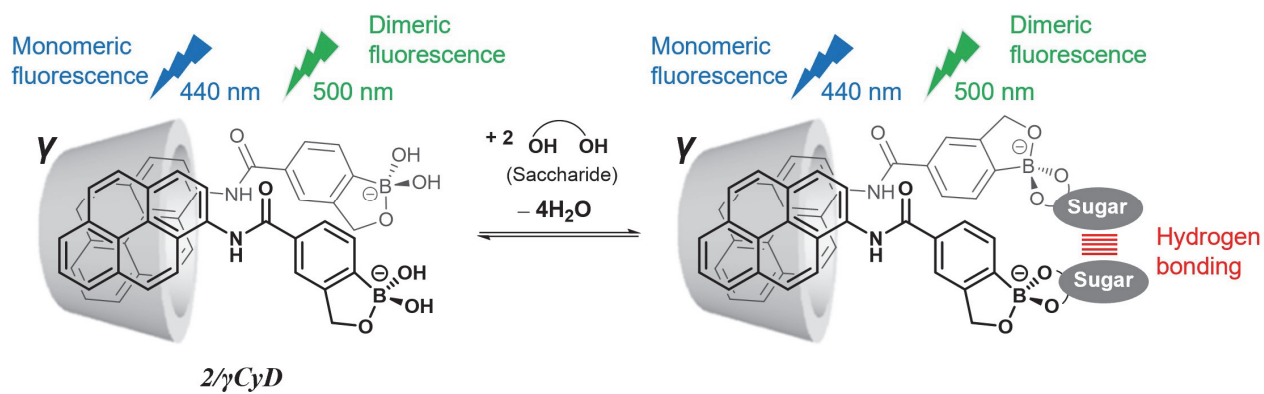
Figure S16-3. UV-vis absorption spectra of *2/γCyD* in the absence and presence of each saccharide (10 mM) in DMSO/water (2/98 in v/v): C_{probe} = 9.99 μM, $C_{\gamma CyD}$ = 5 mM, 10 mM of phosphate buffer, pH = 10.2, T = 25°C, and I = 0.10 M.

Sensing mechanism of *2/γCyD*

Scheme S3. Plausible mechanism for the sensing of saccharides by *2/γCyD*.

Comparison of sensing mechanisms

(a)

Lower pH

pK_a^B

Higher pH

$+ H_2O$ / $- H^+$ K_a^B

Boronic acid

Boronate ion

$- H_2O$ / $- H^+$

Sugar

$- 2 H_2O$

Sugar

Large ratiometric change, Low affinity

Small ratiometric change, **High affinity**
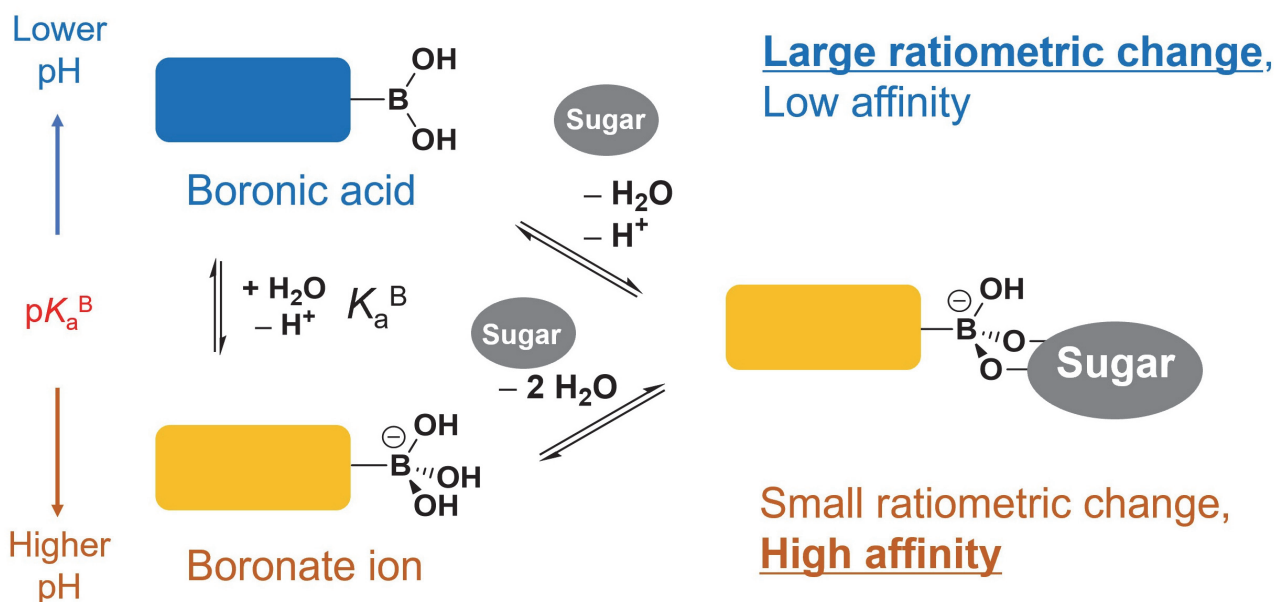
(b)

Dimeric fluorescence
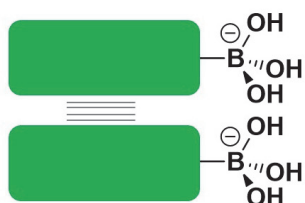
Monomeric fluorescence

Sugar

Large ratiometric change and high affinity for saccharides

Scheme S4. Diagrams describing ratiometric sensing mechanisms of typical boronic acid-based chemosensors (a) and *1/γCyD* (b).

1   C. Priem and A. Geyer, *Chem. Eur. J.*, 2019, **25**, 14278–14283.

2   P. K. Glasoe and F. A. Long, *J. Phys. Chem.*, 1960, **64**, 188–190.

3   Gaussian 16, Revision A.03, M. J. Frisch, G. W. Trucks, H. B. Schlegel, G. E. Scuseria, M. A. Robb, J. R. Cheeseman, G. Scalmani, V. Barone, G. A. Petersson, H. Nakatsuji, X. Li, M. Caricato, A. V. Marenich, J. Bloino, B. G. Janesko, R. Gomperts, B. Mennucci, H. P. Hratchian, J. V. Ortiz, A. F. Izmaylov, J. L. Sonnenberg, D. Williams-Young, F. Ding, F. Lipparini, F. Egidi, J. Goings, B. Peng, A. Petrone, T. Henderson, D. Ranasinghe, V. G. Zakrzewski, J. Gao, N. Rega, G. Zheng, W. Liang, M. Hada, M. Ehara, K. Toyota, R. Fukuda, J. Hasegawa, M. Ishida, T. Nakajima, Y. Honda, O. Kitao, H. Nakai, T. Vreven, K. Throssell, J. A. Montgomery, Jr., J. E. Peralta, F. Ogliaro, M. J. Bearpark, J. J. Heyd, E. N. Brothers, K. N. Kudin, V. N. Staroverov, T. A. Keith, R. Kobayashi, J. Normand, K. Raghavachari, A. P. Rendell, J. C. Burant, S. S. Iyengar, J. Tomasi, M. Cossi, J. M. Millam, M. Klene, C. Adamo, R. Cammi, J. W. Ochterski, R. L. Martin, K. Morokuma, O. Farkas, J. B. Foresman, and D. J. Fox, Gaussian, Inc., Wallingford CT, 2016.

4   GaussView, Version 6, Roy Dennington, Todd A. Keith, and John M. Millam, Semichem Inc., Shawnee Mission, KS, 2016.

5   (a) F. B. T. Pessine, A. Calderini, G. L. Alexandrino, Review: Cyclodextrin inclusion complexes probed by NMR techniques. In *Magnetic Resonance Spectroscopy*, ed. K. Dong-Hyun, Intech, 2012, 237–264. (b) H.-J. Schneider, F. Hacket, V. Rüdiger, H. Ikeda, *Chemical Reviews*, 1998, **98**, 1755–1785.

6   T. Barclay, M. Ginic-Markovic, M. R. Johnston, P. Cooper and N. Petrovsky, *Carbohydr. Res.*, 2012, **347**, 136–141.

7   K. Fukada, T. Ishii, K. Tanaka, M. Yamaji, Y. Yamaoka, K. Kobashi and K. Izumori, *Bull. Chem. Soc. Jpn.*, 2010, **83**, 1193–1197.